VARIATIONAL STUDY OF ${}^{6}_{\Lambda\Lambda}He$ HYPERNUCLEUS AND $\Lambda\Lambda$ POTENTIAL

DISSERTATION

SUBMITTED FOR THE AWARD OF THE DEGREE OF

Master of Philosophy

IN

PHYSICS

BY

ZAFRUL HASAN

Under the Supervision of

Dr. Anisul Ain Usmani

DEPARTMENT OF PHYSICS

ALIGARH MUSLIM UNIVERSITY

ALIGARH (INDIA)

2005-06

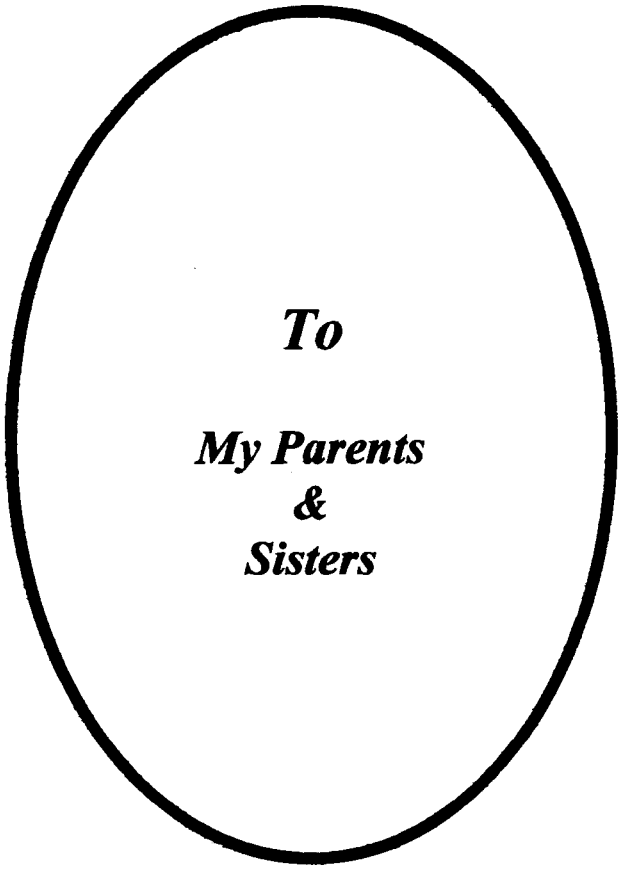
To
My Parents
&
Sisters

Dr. A. A. Usmani
Reader

DEPARTMENT OF PHYSICS
ALIGARH MUSLIM UNIVERSITY
ALIGARH-202 002, INDIA
Phone : Off. +9-1571-2701001
Fax. : +91-571-2701001
Email : **anisul@iucaa.ernet.in**

CERTIFICATE

The research **"Variational Study of ${}^{6}_{\Lambda\Lambda}He$ Hypernucleus and $\Lambda\Lambda$ Potential"**, carried out by Mr. Zafrul Hasan under my supervision is original. The work is suitable for submission for the award of the degree of Master of Philosophy in Physics.

(Dr. Anisul Ain Usmani)

09-01-2006

Acknowledgement

I am grateful to my supervisor Dr. A. A. Usmani by whom the topic for this M. Phil. programme "**Variational Study of** ${}^{6}_{\Lambda\Lambda}He$ **Hypernucleus and** $\Lambda\Lambda$ **Potential**" was concieved. I would like to express my deep sense of gratitude for his inspiring and able guidance, and also for his relentless involvement during the course of this work.

I am thankful to our Chairman, Department of Physics, Prof. Muhammad Irfan who has always been supportive and has provided me all the facilities required to materialize this dissertation work. I am immensely thankful to the staff of seminar library for providing me the required journals during my research work. I am very grateful to my family and my friends who always have been helpful and supportive.

Zafrul Hasan 9/1/2006

Contents

Chapter 1

Introduction

A hypernucleus is a nuclear species formed when at least one strange baryon e.g. Λ, Σ or Ξ get trapped in a core nucleus which may be ordinarily stable or unstable, thus forming a short lived nuclear system. Historically, first Λ- hypernucleus was observed in 1953s by Polish scientist Danysz and Pniewsky in a balloon flown emulsion stack exposed to cosmic ray at high altitude [1]. This initial cosmic ray observation of hypernuclei were followed by pion and proton beam production in emulsions and then ^4He bubble chambers. Later on many single-hypernuclei [2] and three double-Λ hypernuclei were reported [3, 4, 5]. Symbolically, single-hypernuclei are represented by ${}^{A}_{Y}Z$, where A is total number of baryons and Y means hyperon (may be Λ, Σ, or Ξ). A double-Λ hypernuclus is represented by ${}_{YY}^{A}Z$, where Y is Λ hyperon and A total number of baryons. A Λ-hyperon is unstable in free space and it interacts with nucleons through strong interaction $\Lambda N \rightarrow \Lambda N$ with a life time of 10^{-22} sec. The free space properties of the hyperon need not necessarily be the same as bound state properties. It is established fact that binding effect lengthen this life time to the order of 10^{-10} seconds.

In the strangeness nuclear physics, the most fundamental problem is to recognize various facets of interactions among octet baryons (N, Λ, Σ, Ξ) in a unified way.

Table 1.1: Experimental double-Λ hypernuclei binding energies, $B_{\Lambda\Lambda}$ and the values of the quantity $\Delta B_{\Lambda\Lambda}$ ($\Delta B_{\Lambda\Lambda} = B_{\Lambda\Lambda}({}^{A}_{\Lambda\Lambda}Z) - 2B_{\Lambda}({}^{A-1}_{\Lambda}Z)$).

Double-Λ hypernucleus	$B_{\Lambda\Lambda}$ (MeV)	$\Delta B_{\Lambda\Lambda}$(MeV)
${}^{6}_{\Lambda\Lambda}He$	$10.9^{+}_{-}0.8$	$4.7^{+}_{-}1.0$
${}^{10}_{\Lambda\Lambda}Be$	$17.7^{+}_{-}0.4$	$4.3^{+}_{-}0.4$
${}^{13}_{\Lambda\Lambda}B$	$27.5^{+}_{-}0.7$	$4.8^{+}_{-}0.7$

Our detailed knowledge for the $S = 0$ (strangeness 0) NN sector is based on the rich data of NN scattering as well as nuclear phenomenon. Recent studies for $S = -1$ many-body systems such as Λ hypernuclei have clarified interesting features of ΛN and ΣN interactions in spite of scarce data of the free space scattering. On the other hand, for baryon-baryon interactions with $S = -2$ sector, concerned presently, experimental information has been highly limited due to the extreme difficulties of two-body scattering experiments. Therefore, the observed ΛΛ bond energies of double-Λ hypernuclei should be the most reliable source for the $S = -2$ interaction, and such data pay a decisive role in determining the strength of underlying Λ-Λ interaction.

Thus the doubly strange ΛΛ and Ξ hypernuclei provide the primary data that address the question of the properties of the $S = -2$ Λ-Λ interaction both inside the nuclear medium and in the vacuum. Direct two-body scattering is impractical due to the lack of targets, so the data on ΛΛ hypernuclei provide a unique method to learn details on the Λ-Λ interaction in the vacuum. Since, the double-Λ hypernuclei are discovered, effort to extract the medium as well as vacuum Λ-Λ interaction from these systems are made by many authors, among them few are Danysz, Prowse, Aoki etc.. The detailed history of Λ-Λ interaction given by these authors from 1960s to till now is presented in Table 1.1 and Fig. 1.1.

Although, these are identified as double-Λ hypernuclei, we can not exclude a possibility of H-nuclear state or hyperon mixed state among baryon octet. This is also a problem of great interest because we know only the binding energy [7]. If the mass of

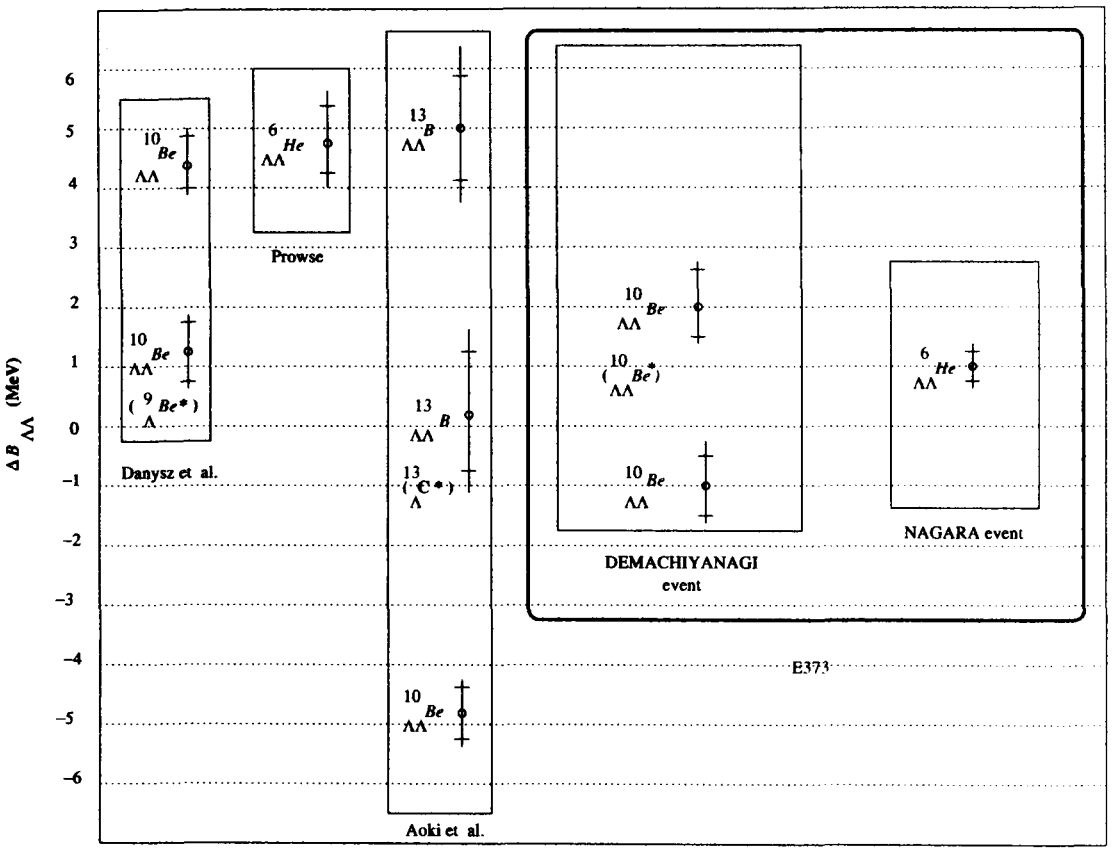

Figure 1.1: The summary of experimental values of $\Delta B_{\Lambda\Lambda}$. As for the NAGARA event, the indicated error bar does not include the uncertainty of the binding energy of the Ξ^- hyperon.

the H dibaryon, M_H is less than Λ hyperon mass in the nucleus, two Λ hyperon in the nucleus would be expected to form the H dibaryon. With this assumption the lower limit of the mass of the H dibaryon can be calculated from the following relation

$$M_H > 2M_\Lambda - B_{\Lambda\Lambda},$$

where M_Λ is the mass of a Λ hyperon in free space and $B_{\Lambda\Lambda}$ is separation energy of two Λ hyperons from core nucleus.

The data of the NAGARA event indicate four possibilities on the YN and YY interactions as follows:

1. weakly attractive Λ-Λ interaction with weak $\Lambda\Lambda$- ΞN- $\Sigma\Sigma$- coupling effect,

2. almost zero or weak repulsive Λ-Λ interaction with moderate $\Lambda\Lambda$- ΞN- $\Sigma\Sigma$- coupling effect,

3. repulsive Λ-Λ interaction with strong $\Lambda\Lambda$- ΞN- $\Sigma\Sigma$- coupling effect and

4. $\Lambda\Lambda$- ΞN- $\Sigma\Sigma$- as strong as to produce weakly bound or resonant H dibaryon state.

Strangeness degree of freedom brings subtle distortions to the properties and symmetries of a bound nucleus. How things behave with the injection of different quanta of strangeness constitutes a study of great importance. We have three well established double-Λ hypernuclear species (${}^{10}_{\Lambda\Lambda}Be$, ${}^{6}_{\Lambda\Lambda}He$, ${}^{13}_{\Lambda\Lambda}B$) [3, 4, 5] and to study along with large number of single-Λ hypernuclei. Fortunately, experimental data for ${}^{6}_{\Lambda\Lambda}He$ ($S = -2$) and ${}^{5}_{\Lambda}He$ ($S = -1$) bound with the same core nucleus ${}^{4}He$ ($S = 0$) are available with reasonable statistics for a successful theoretical estimate. The observation of ${}^{6}_{\Lambda\Lambda}He$ event in KEK hybrid experiment [8] E373, called the NAGARA event, and the evidence for bound ${}^{4}_{\Lambda\Lambda}H$ ($I = 0$, $J = 1^+$) observed through (K^-, K^+) reaction on ${}^{9}Be$ target in the Brookhaven alternating-gradient synchrotron experiment E906 [9], have given fresh impetus to the field of hypernuclei in the $S = -2$ sector on both theoretical and experimental frontiers. Although there are only three established double-hypernuclear species [3, 4, 5, 8, 9], theoretical side is growing with a fast

pace. For example, cluster model analysis using Faddeev-Yakubovsky (FY) method by Flikhin and Gal [10, 11, 12], Flikhin, Gal and Suslov [13] and by Yamamoto et al. [14] are notable. These studies together lead to an inconsistence picture of the experimental data as discussed at length in the Variational Monte Carlo (VMC) study of ${}^{6}_{\Lambda\Lambda}He$ by Shoeb [15]. This study is performed with central potentials and correlations and hence is far from the realistic description of the nuclear system. Another study by Usmani, Bodmer and Sharma [16] is performed ignoring ΛN space-exchange correlation (SEC) in the wave function and therefore is deficient. This is because SEC is an important correlation, which being quite significant at $r < 2.0$ fm , affects each and every piece of energy breakdown of the hypernucleus, Λ-separation energy (B_Λ), nuclear core polarization, point proton radius and density profiles as shown in a very recent study by Usmani [17] of ${}^{5}_{\Lambda}He$ hypernucleus performed using a realistic Hamiltonian and a fully correlated wave function that takes into account all relevent dynamical correlations along with SEC. The other studies which include SEC are Faddeev-Yakubovsky (FY) calculations of ${}^{4}_{\Lambda}H$ and ${}^{4}_{\Lambda}He$ by Nogga et al. [18], yet to be extended to five- and six- body hypernuclei, and Green's Function Monte Carlo (GFMC) calculations of s-shell single hypernuclei by Nemura et al. [19]. As SEC is naturally inbuilt in their formalism, its effect can not be deduced directly as done for ${}^{5}_{\Lambda}He$ in Ref. [17] and for ${}^{6}_{\Lambda\Lambda}He$ in this study. The significant SEC effects observed for ${}^{5}_{\Lambda}He$ may manifest more in ${}^{6}_{\Lambda\Lambda}He$ because of the presence of a pair of Λ hyperon. It also implicates various subtle issues, like the physical existence of a bound ${}^{4}_{\Lambda\Lambda}H$, SU(3) symmetry breaking of baryon-baryon (BB) potential and the question whether we can successfully produce the hypernuclear energy spectra using realistic BB and three baryon ($3B$) interactions without including the underlying Quantum Chromodynamics (QCD). Findings of ${}^{5}_{\Lambda}He$ suggests that addressing these issues without SEC would hopelessly be deficient.

The dissertation is organised in six chapters. Chapter 1 is the introduction. In Chapter 2, we present details of production mechanism and interpretation of reported three double-Λ hypernuclei ${}^{10}_{\Lambda\Lambda}B$, ${}^{6}_{\Lambda\Lambda}He$ and ${}^{13}_{\Lambda\Lambda}Be$. In Chapter 3 and 4, we discuss Hamiltonian of A baryon double-Λ hypernuclei and Variational Wave Function, re-

spectively. In Chapter 5, we briefly discuss Variational Monte Carlo method. Finally, the results are discussed in Chapter 6.

Chapter 2

Production and Interpretation of Double-Λ Hypernuclear Events

In principle, any interaction occuring within a complex nucleus and capable of producing two Λ hyperons may give rise to the formation of a double-Λ hypernucleus. The production of double-Λ hypernuclei become possible with the advent of separated K^- meson beam accelerator at BNL, CERN and KEK. This meson beam is used to tag the production of the Ξ^- hyperon, which is then slowed down in emulsion and captured at rest (Fig. 2.1). The elementary processes are

$$K^- + p \rightarrow K^+ + \Xi^- \tag{2.1}$$

$$\Xi^- + p \rightarrow \Lambda + \Lambda + 28 \text{ MeV} \tag{2.2}$$

The proton in process (2.2) is embedded in an emulsion nucleus (^{12}C, ^{14}N, ^{16}O or heavier). With such a small energy release, it is correspondingly probable that the two Λ particles will be trapped in the absorbing nucleus (i.e. a nuclear structure containing two bound Λ hyperons), leading to either two ordinary hypernuclei or one double-Λ hypernucleus, even for the case of capture by the light emulsion nuclei. The production and subsequent cascade decay of double hyperfragment will be recorded in emulsion.

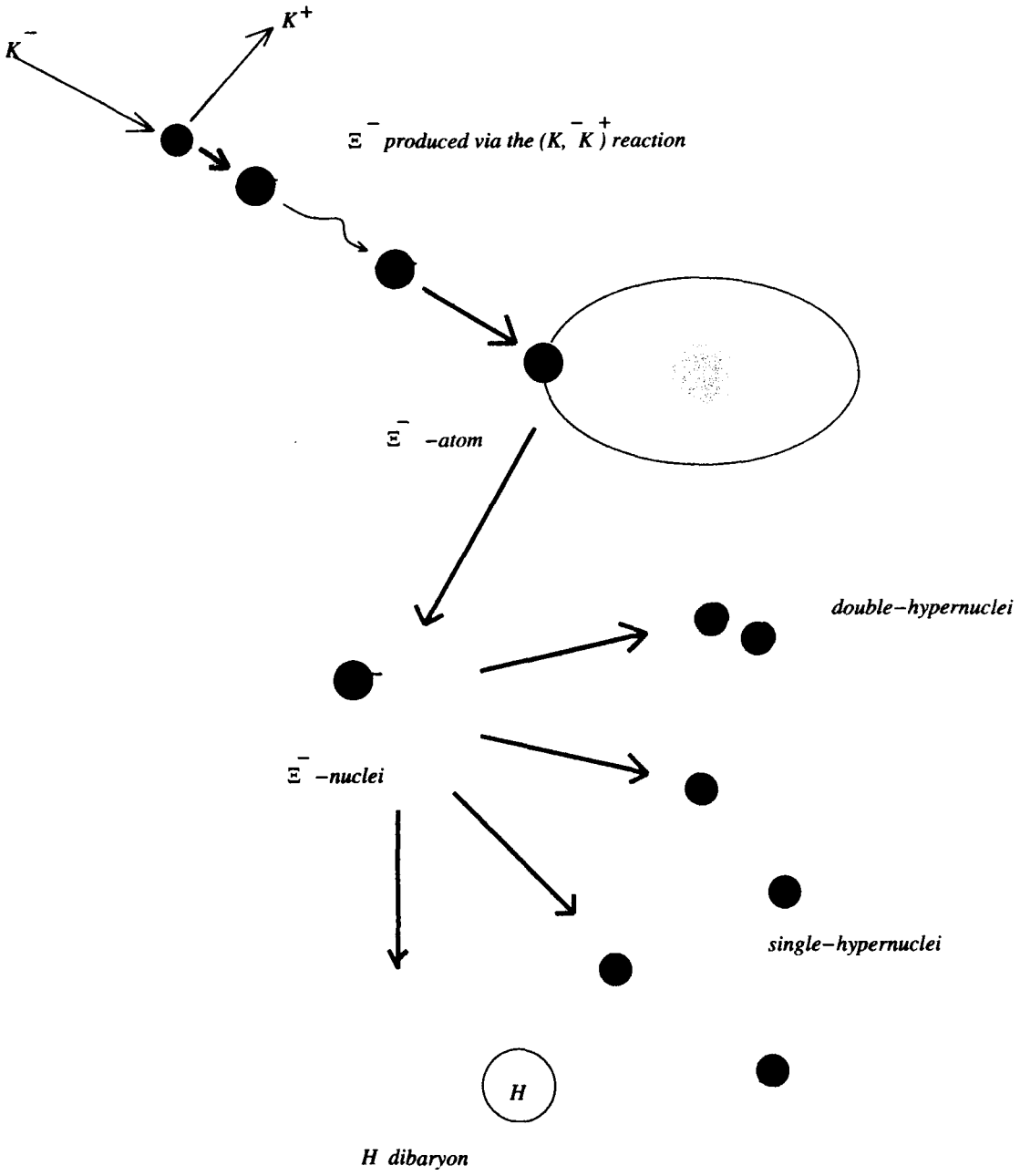

Figure 2.1: Production process of double-hypernuclei, single-hypernuclei, and the H dibaryon.

In general, the ranges of both the double hyperfragment and the ordinary hyperfragment resulting from its decay will be so short that the detection and analysis of such an event may present difficulties. In particular, for carbon and oxygen, where the separation energy of the proton is large, 16 and 12 MeV, respectively, the Q value for reaction (2.2) is reduced substantially in light emulsion nuclei. A double-Λ hypernucleus ${}^{A}_{\Lambda\Lambda}Z$, which is a composite system of nuclear core ${}^{A-2}Z$ and two bound Λ particles. The quantity $B_{\Lambda\Lambda}$ is defined as the total binding energy of the double-Λ hypernucleus, and it is given by

$$B_{\Lambda\Lambda} = -\left[M({}^{A}_{\Lambda\Lambda}Z) - M({}^{A-2}Z) - 2m_{\Lambda}\right], \tag{2.3}$$

where M denotes mass of the system which appears inside the brackets and m_{Λ} (1115.6 MeV) is the Λ mass. The $\Lambda\Lambda$ bond energy $\Delta B_{\Lambda\Lambda}$ in double-Λ hypernuclei is determined experimentally from the measurement of binding energy of double- and single-Λ hypernuclei as

$$\Delta B_{\Lambda\Lambda} = B_{\Lambda\Lambda}({}^{A}_{\Lambda\Lambda}Z) - 2B_{\Lambda}({}^{A-1}_{\Lambda}Z), \tag{2.4}$$

where $B_{\Lambda}(> 0)$, is given by

$$B_{\Lambda} = -\left[M({}^{A-1}_{\Lambda}Z) - M({}^{A-2}Z) - m_{\Lambda}\right], \tag{2.5}$$

is the binding energy of a Λ hyperon in the hypernucleus ${}^{A-1}_{\Lambda}Z$.

Historically, in the 1960s two double-Λ hypernuclei, ${}^{10}_{\Lambda\Lambda}Be$ [3] and ${}^{6}_{\Lambda\Lambda}He$ [4] were reported in emulsion experiments, but the reality of the later case is considered doubtful [21]. Two decades later the modern emulsion-counter hybrid technique has been applied in the KEK-E176 experiment [5], in which a new double-Λ hypernuclear event was found but no unique identification was given so for: One explanation as ${}^{10}_{\Lambda\Lambda}Be$ leads to a repulsive Λ-Λ interaction ($\Delta B_{\Lambda\Lambda} < 0$), while the other possibility involving ${}^{13}_{\Lambda\Lambda}B$ leads to an attractive Λ-Λ interaction [22, 23]. If the later is the case, the extracted strength of the Λ-Λ interaction is attractive with $\Delta B_{\Lambda\Lambda} \approx 4$ MeV. Although the later option seems consistent with the old data of ${}^{10}_{\Lambda\Lambda}Be$ [3], the substantially attractive Λ-Λ interaction has not been convincing. The ${}^{6}_{\Lambda\Lambda}He$ double-hyperfragment also has been

confirmed experimentally with more precise values of $B_{\Lambda\Lambda}$ and $\Delta B_{\Lambda\Lambda}$ in a hybrid emulsion experiment (KEK-E373 experiment) in 2001 [8], this event is known as NAGARA event.

2.1 Interpretation of ${}^{10}_{\Lambda\Lambda}Be$ Hypernucleus

(DEMACHIYANAGI event)

The first double-hyperfragment ${}^{10}_{\Lambda\Lambda}Be$ is observed during a systematic scan for interactions of 1.3- and 1.5-Gev/c mesons in emulsion irradiated in the separated K^- meson beam at CERN, a unique example of the production and subsequent cascade decay of a double hyperfragment has been found.

A schematic drawing of the event is shown in Fig. 2.2. A Ξ^- hyperon (track 1) emitted from the interaction of a K^- meson of momentum 1.5 Gev/c (star A) comes to rest and is absorbed at B. A double-hyperfragment (track 6) and another charged particle (track 5) are observed to come from star B. The double-hyperfragment decays at C into the π^- meson (track 7), a singly charged particle (track 8), and an ordinary hyperfragment (track 9). This hyperfragment decays at D into a π^- meson (track 10) and three other charged particles (tracks 11, 12, and 13). The results of the measurements of the angles of emission and ranges of all the charged particles track involved in these processes give reasonable interpretation of the event.

The ordinary hyperfragment is analyzed using only the kinematics of its decay, where as the possible identities and decay schemes of the double-hyperfragment are assigned from a study of both the production and decay processes. The analysis of final results are summarized in Table 1 [24].

From the comparison of the binding energies $B_{\Lambda\Lambda}$ of the two Λ-hyperons in double-hyperfragments with B_Λ for ordinary hyperfragments, one can expect to obtain information not only on the strength of the Λ-Λ interaction but also on the spin-dependent part of the binding energy in ordinary hyperfragments. The value of the $\Delta B_{\Lambda\Lambda}$ presented in Table 1, column 7, is the net contribution of the Λ-Λ interaction and the reduction due to the spin-dependent part of the Λ-core distortion effects may be ne-

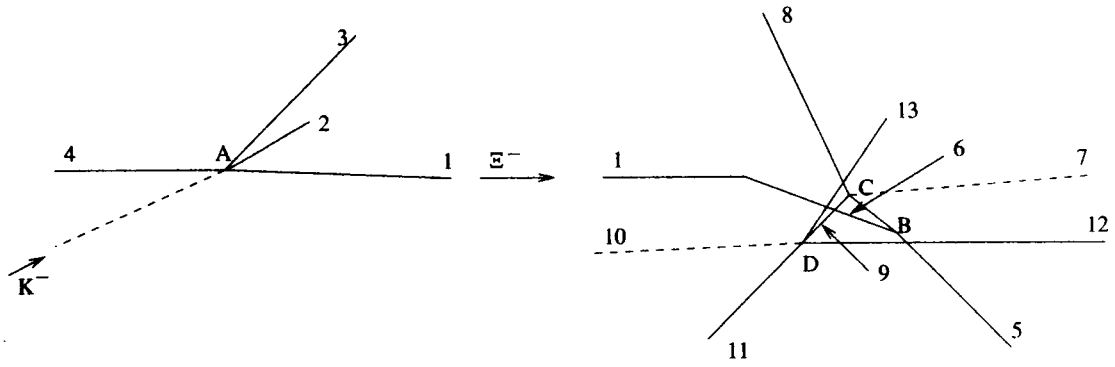

Figure 2.2: A schematic drawing of the production of a Ξ^- hyperon in a 1.5 GeV/c K^--meson interaction at A. This Ξ^- hyperon is captured at B with the emission of a double-hyperfragment decaying in cascade at C and D.

glected. In the case of ${}^{10}_{\Lambda\Lambda}Be$, when the spin of the core is zero, $\Delta B_{\Lambda\Lambda}$ gives the contribution of the Λ-Λ interaction alone. In the case of ${}^{11}_{\Lambda\Lambda}Be$, the spin of the core differs from zero, and the spin dependent part of the Λ-core interaction must be taken into account.

Arguments based on consideration of the production and decay of the double-hyperfragments Table 1, suggest that the most likely explanation of the whole sequence of events is the production of a ${}^{10}_{\Lambda\Lambda}Be$ or ${}^{11}_{\Lambda\Lambda}Be$ by a Ξ^- hyperon capture on carbon followed by the decay sequences shown in Table 1 by row 1 and 3. The most possible double hyperfragment is ${}^{10}_{\Lambda\Lambda}Be$, because the values of $B_{\Lambda\Lambda}$ and $\Delta B_{\Lambda\Lambda}$ is much close to old data.

Therefore, the accepted production and decay sequence of ${}^{10}_{\Lambda\Lambda}Be$ hypernucleus is:

$$\Xi^- + {}^{12}C \rightarrow {}^{10}_{\Lambda\Lambda}Be + t \tag{2.6}$$

$${}^{10}_{\Lambda\Lambda}Be \rightarrow {}^{9}_{\Lambda}B + p + \pi^- \tag{2.7}$$

$${}^{9}_{\Lambda}B \rightarrow 2\ {}^{4}He + p + \pi^- \tag{2.8}$$

with $\quad \Delta B_{\Lambda\Lambda} = +4.5^{+}_{-}0.4$ MeV.

Table 1: Summary of results

Star C decay mode of double HF	$B_{\Lambda}(_{\Lambda\Lambda}Z)$MeV	Star D decay mode of single HF	$B_{\Lambda}(_{\Lambda}Z)$MeV	Δp (MeV/c)	$B_{\Lambda\Lambda}$(MeV)	$\Delta B_{\Lambda\Lambda}$(MeV)
$^{10}_{\Lambda\Lambda}Be \rightarrow {}^{9}_{\Lambda}Be + {}^{1}H + \pi^-$	11.0 ± 0.4	$^{9}_{\Lambda}Be \rightarrow 2\,{}^{4}_{\Lambda}He + {}^{1}H + \pi^-$	7.2 ± 0.6	20 ± 12	17.5 ± 0.4	4.5 ± 0.4
$^{11}_{\Lambda\Lambda}Be \rightarrow {}^{9}_{\Lambda}Be + {}^{1}H + n + \pi^-$	$< 7.6 \pm 0.7$	$^{9}_{\Lambda}Be \rightarrow 2\,{}^{4}_{\Lambda}He + {}^{1}H + \pi^-$	7.2 ± 0.6	20 ± 12	$< 16.5 \pm 0.4$	$< -0.3 \pm 1.0$
$^{11}_{\Lambda\Lambda}Be \rightarrow {}^{10}_{\Lambda}Be + {}^{1}H + \pi^-$	11.1 ± 0.4	$^{10}_{\Lambda}Be \rightarrow 2\,{}^{4}_{\Lambda}He + {}^{2}H + \pi^-$	7.5 ± 0.6	17 ± 12	19 ± 0.6	3.2 ± 0.6
$^{8}_{\Lambda\Lambda}Li \rightarrow {}^{7}_{\Lambda}Li + {}^{1}H + \pi^-$	10.8 ± 0.4	$^{7}_{\Lambda}Li \rightarrow {}^{4}_{\Lambda}He + {}^{2}H + {}^{1}H + \pi^-$	6.5 ± 0.6	40 ± 14	16.3 ± 0.4	5.3 ± 0.4
$^{9}_{\Lambda\Lambda}Li \rightarrow {}^{8}_{\Lambda}Li + {}^{1}H + \pi^-$	10.9 ± 0.4	$^{8}_{\Lambda}Li \rightarrow {}^{4}_{\Lambda}He + {}^{3}H + {}^{1}H + \pi^-$	5.4 ± 0.6	27 ± 15	17.3 ± 0.4	4.4 ± 0.4
$^{10}_{\Lambda\Lambda}Li \rightarrow {}^{8}_{\Lambda}Li + {}^{1}H + n + \pi^-$	$< 7.5 \pm 0.5$	$^{8}_{\Lambda}Li \rightarrow {}^{4}_{\Lambda}He + {}^{3}H + {}^{1}H + \pi^-$	5.4 ± 0.6	27 ± 15	$< 15.5 \pm 0.4$	$- < 0.5 \pm 0.6$

2.2 Interpretation of ${}^{13}_{\Lambda\Lambda}B$ Hypernucleus

Long after the discoveries of two double-Λ hypernuclei, ${}^{6}_{\Lambda\Lambda}He$ and ${}^{10}_{\Lambda\Lambda}Be$ (one event each), in Ξ^- capture at rest in emulsion in 1960s , the event ${}^{10}_{\Lambda\Lambda}Be$ has also been reanalyzed in detail by Dalitz et al.[26], and the original interpretation remains sound. Recently, new experiments [5, 25] have been carried out at KEK Proton Syncrotron in Japan with a 1.66 GeV/c beam of K^- mesons, a new species of double-Λ hypernucleus is interpreted as ${}^{10}_{\Lambda\Lambda}Be$ or ${}^{13}_{\Lambda\Lambda}B$. However, the possibility of the single- or double-hypernuclear production in excited states is ignored in the analysis. The schematic drawing of the double-Λ hypernuclear event of Aoki et al. is shown in Fig. 2.3. The interpretation is given by these authors in terms of the formation and decay of ${}^{10}_{\Lambda\Lambda}Be$ or ${}^{13}_{\Lambda\Lambda}B$. For the former, the reaction chain is hypothesized to be as follows (A, B, C refers to the vertices in Fig. 2.3):

$$\text{A}: \quad \Xi^- + {}^{12}C \rightarrow {}^{10}_{\Lambda\Lambda}Be + {}^{3}H, \tag{2.9}$$

$$\text{B}: \quad {}^{10}_{\Lambda\Lambda}Be \rightarrow \pi^- + {}^{10}_{\Lambda}B, \tag{2.10}$$

$$\text{C}: \quad {}^{10}_{\Lambda}B \rightarrow {}^{3}He + {}^{4}He + 2n \quad \text{etc.} \tag{2.11}$$

From above processes, the binding energy $B_{\Lambda\Lambda}({}^{A}_{\Lambda\Lambda}Z)$ =M(^{A-2}Z) $+2M_\Lambda$ - M($^{A}_{\Lambda\Lambda}Z$) is calculated which is found to be 8.5±0.7 MeV, and $\Delta B_{\Lambda\Lambda}$ ($^{A}_{\Lambda\Lambda}Z$) =$\Delta B_{\Lambda\Lambda}$- $2B_{\Lambda\Lambda}$ ($^{A-1}_{\Lambda}Z$) is found to be -4.9±0.7 MeV (B_Λ=6.71±0.04 MeV is the Λ-binding energy in ${}^{9}_{\Lambda}Be$). This minus sign implies a repulsive Λ-Λ interaction, which does not agrees with the values $B_{\Lambda\Lambda}$=17.7±0.4 MeV and $\Delta B_{\Lambda\Lambda}$=4.3±0.4 MeV as obtained by Dalitz et al. [26] for ${}^{10}_{\Lambda\Lambda}Be$; in this case the Λ-Λ interaction is attractive. Thus rejecting the formation of event ${}^{10}_{\Lambda\Lambda}Be$. Therefore, event is ${}^{13}_{\Lambda\Lambda}B$ not ${}^{10}_{\Lambda\Lambda}Be$, the interpretation of ${}^{13}_{\Lambda\Lambda}B$ event is given by proposing that the formation is via an intermediate excited state of ${}^{14}_{\Lambda\Lambda}C^*$. In this interpretation, the reaction processes are:

$$\text{A}: \quad \Xi^- + {}^{14}N \rightarrow n + {}^{14}_{\Lambda\Lambda}C^* \rightarrow n + p + {}^{13}_{\Lambda\Lambda}B \tag{2.12}$$

$$\text{B}: \quad {}^{13}_{\Lambda\Lambda}B \rightarrow \pi^- + {}^{13}_{\Lambda}C \tag{2.13}$$

$$\text{C}: \quad {}^{13}_{\Lambda}C \rightarrow {}^{3}He + {}^{4}He + {}^{4}He + 2n \quad \text{etc.} \tag{2.14}$$

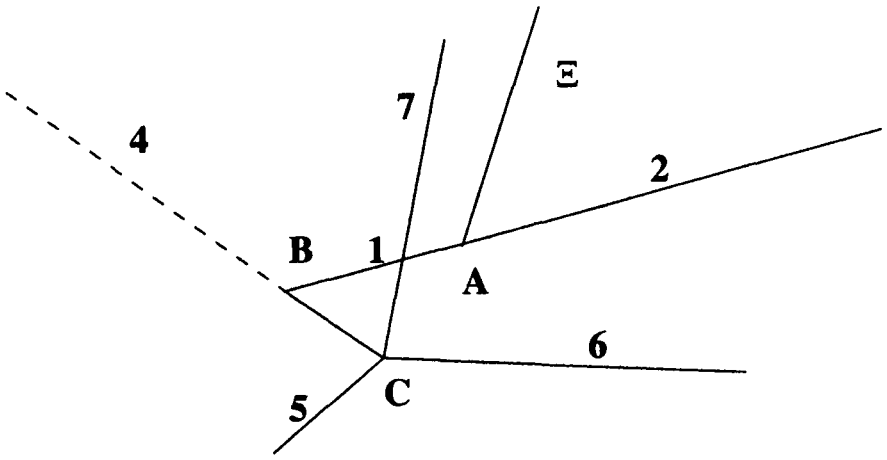

Figure 2.3: The schematic drawing of the double-Λ hypernuclear event of Aoki et al. [5]. The vertices A, B and C correspond to production via Ξ^- capture, pionic weak decay of the double-Λ hypernucleus, and nonmesonic weak decay of a single-Λ hypernucleus respectively.

The vertex A in this interpretation corresponds to a sequence of two-body decays, proceeding through a relatively long-lived excited state

$$^{14}_{\Lambda\Lambda}C^* \approx s_\Lambda p_\Lambda \otimes^{12} C^*(T=1)$$

consisting of Λ's in s- and p-wave shell-model orbitals. This interpretation outlined in Eqn. 2.12 - 2.13 gives $B_{\Lambda\Lambda}$=27.5$\pm$0.7 MeV and $\Delta B_{\Lambda\Lambda}$=4.8$\pm$0.7 MeV that agrees with Prowse, Danysz et al. and Dalitz et al. [3, 4, 26].

Now, we present arguments supporting our interpretation. These include

1. kinematics of the observed charged particle tracks and consistency with energy momentum coservation;
2. reaction mechanism for double-Λ hypernuclear production from Ξ^- atoms;
3. hypernuclear decay mode.

2.2.1 Kinematics

An interpretation of the event in terms of the formation of a specific double hypernucleus ${}^{A}_{\Lambda\Lambda}Z$ must consistently satisfy energy and momentum conservation at the production vertex A and the mesonic decay vertex B. The tracks 3 and 4 are collinear at the mesonic decy vertex B i.e. a two-body decay. For two-body decay ${}^{A}_{\Lambda\Lambda}Z \rightarrow \pi^- + {}^{A}_{\Lambda}(Z+1)$ to the ground state of single hypernucleus, the mass of the double hypernucleus is

$$M({}^{A}_{\Lambda\Lambda}Z) = M^{A}_{\Lambda}(Z+1) + E_{\pi} + \frac{p^2_{\pi}}{2M({}^{A}_{\Lambda}(Z+1))} \tag{2.15}$$

The value of $B_{\Lambda\Lambda}$ which results is an upper limit since the single hypernucleus could have been produced in an excited state which generally results in an unobserved γ ray.

The $B_{\Lambda\Lambda}$ obtained from the mesonic decay can be used to calculate the Q value for production reaction involving the capture of a Ξ^- on ${}^{12}C$, ${}^{14}N$ or ${}^{16}O$, for valid fit, kinetic energies should sum to Q value. From the mesonic decay given in Eqn. 2.12, we get B_{Λ} (${}^{13}_{\Lambda}C$)=11.69$\pm$0.12 MeV [27], $B_{\Lambda\Lambda}({}^{13}_{\Lambda\Lambda}B)$=27.5$\pm$0.7 MeV (and $\Delta B_{\Lambda\Lambda}$=4.8$\pm$0.7MeV) which then implies a Q value of 27.5$\pm$0.7 MeV for the production reaction $\Xi + {}^{14}N \rightarrow n + p + {}^{13}_{\Lambda\Lambda}B$. The momentum conservation at vertex A with T_p=5.28 MeV and T_B=3.4 MeV, we obtain T_n=19.7 MeV and an energy release of E_{sum}=28.4 MeV with a typical error of 1-2 MeV, which is much close to Q value to make ${}^{13}_{\Lambda\Lambda}B$ a kinematically acceptable candidate for the double hypernucleus. T_n increases by 0.9 MeV for a 0.1 MeV increase in the kinetic energy of the double hypernucleus. Thus, T_B=3.3 MeV gives T_n=18.8 MeV and E_{sum}=27.4 MeV for an exact match with the Q value.

2.2.2 Reaction Mechanism

We have seen the production of the double-Λ hypernucleus is through a two-body $\Xi^- + p \rightarrow \Lambda + \Lambda$ process, with a short-range form factor dominated by K and K^* exchange, in this process Ξ^- is captured from an atomic orbit with orbital angular momentum l_{Ξ} while proton occupies an orbit l_p, the produced double-Λ hypernucleus will be in ground state if $l_{\Xi} = l_p$. This selection rule [28] implies that excited state will be preferentially populated when a Ξ^- is captured in an emulsion nucleus.

2.2.3 Hypernuclear Decay Mode

In Fig. 2.3, the vertex B corresponds to the emission of energetic pions, at this vertex produced hypernucleus will be in ground state but we can not exclude the production of low-lying excited state, followed by γ emission to the ground state. The weak decay process at vertex C does not give enough information, by the way the process is irrelevant to our interpretation of double-Λ hypernuclear event.

2.3 Interpretation of ${}^{6}_{\Lambda\Lambda}He$ Hypernucleus

(NAGARA event)

Although people have analyzed only 32% of the total emulsion and have found an event of seminal importance, a mesonically decaying double-Λ hypernucleus in ground state emitted from a Ξ^- hyperon capture at rest. A schematic drawing of the event is shown in Fig. 2.4, this event is known as "NAGARA" event. A Ξ^- hyperon came to rest at point A, from which three charged particles (track 1, 3 and 4) are emitting. One of them decayed into a π^- meson (track 6) and two other charged particles (track 2, 5) at point B. The particle of track 2 decays again into two charged particles (tracks 7, 8) at point C. The measured lengths and emission angles of these tracks are summarized in Table 2.1.

The single-hypernucleus (track 2) isidentified from event reconstruction of its decay at point C. Mesonic decay modes of single-hypernuclei are rejected because their Q values are too small. The decay mode of the single-hypernucleus is non mesonic with neutron emission. If either track 7 or 8 has more than unit charge, the total kinetic energy of the two charged particles is much larger than the Q value of any possible decay mode because of the long ranges of track 7 and 8. Therefore, both track 7 and 8 are singly charged, and only ${}_{\Lambda}He$ isotopes are acceptable.

The kinematics of all possible decay modes of the double hypernucleus (track 1) which decays into ${}_{\Lambda}He$ (track 2) and π^- (track 6) are checked, and $B_{\Lambda\Lambda}$ and $\Delta B_{\Lambda\Lambda}$ are calculated. Since track 5 ended in the base film, only the lower limit of the kinetic

energy can be determined. For the decay modes without neutron emission, the range of the particle of track 5 is increased to minimize the missing momentum. If the sum of the momenta of the three charged particles (track 2, 5 and 6) deviated from zero by more than 3 standard deviations even after the range of track 5 is increased from the missing momentum, that decay mode is rejected. For the decay modes with neutron emission, the upper limits of $B_{\Lambda\Lambda}$ and $\Delta B_{\Lambda\Lambda}$ are obtained. Only the results for $\Delta B_{\Lambda\Lambda} > -20$ MeV are listed in Table 2.2. The case of double hypernuclei with more than two units of charge are not given because their values of $\Delta B_{\Lambda\Lambda}$ are less than -20 MeV.

Kinematical analysis of the production reaction is made by assuming the Ξ^- hyperon is captured by a light nucleus in the emulsion (^{12}C, ^{14}N or ^{16}O). This assumption is reasonable, taking into account the existence of the short track 3 and the column barrier of target nucleus. For each of the modes without neutron emission, if the sum of momenta deviated from zero by more than 3 standard deviations, the mode is rejected. For the modes with one neutron emission, the momentum of the neutron is assigned to the missing momentum of the three charged particles (track 1, 3 and 4). For the modes with more than one neutron emission, the lower limits of the total kinetic energy of the neutrons are calculated from the missing momentum. The results for $\Delta B_{\Lambda\Lambda} < 20$ MeV are presented in Table 2.3. The values of $B_{\Lambda\Lambda}$ and $\Delta B_{\Lambda\Lambda}$ are calculated with the Ξ^- hyperon binding energy B_{Ξ^-} set to zero. Hence these values are lower limits of $B_{\Lambda\Lambda}$ and $\Delta B_{\Lambda\Lambda}$, and their true values are large, depending on the actual value of B_{Ξ^-}.

$$B_{\Lambda\Lambda} = 7.13 + 0.87 B_{\Xi^-} \pm 0.19 \text{ MeV}, \tag{2.16}$$

$$\Delta B_{\Lambda\Lambda} = 0.89 + 0.87 B_{\Xi^-} \pm 0.20 \text{ MeV}. \tag{2.17}$$

A comparison of the values of $B_{\Lambda\Lambda}$ and $\Delta B_{\Lambda\Lambda}$ obtained from both point A and B is made. After rejecting the modes which have inconsistent values, only one interpretation remained, which is given below:

$$\Xi^- + {}^{12}C \rightarrow {}^{6}_{\Lambda\Lambda}He + {}^{4}He + t \tag{2.18}$$

$$ {}^{6}_{\Lambda\Lambda}He \rightarrow {}^{5}_{\Lambda}He + p + \pi^{-} \tag{2.19} $$

$$ {}^{5}_{\Lambda}He \rightarrow p + d + 2n \ etc. \tag{2.20} $$

The fact that the tracks of the reaction products are coplaner at both points A and B also suggests that no neutrons are emitted from either vertex. The decay mode of ${}^{5}_{\Lambda}He$ is non-mesonic but not uniquely determined.

The possibilities that the double-hypernucleus or the single-hypernucleus is produced in an excited state can be rejected for the following reasons. If the double hypernucleus or the other hyperfragments emitted from the Ξ^{-} stopping point has been produced in an excited state, the value of $\Delta B_{\Lambda\Lambda}$ calculated at the production point A would be increased by the excitation energy. On the other hand, if the single-hypernucleus or the residual particles emitted from the decay of the double hypernucleus has been created in an excited state, the value of $\Delta B_{\Lambda\Lambda}$ calculated at the decay point B would be enlarged and the consistency of the values of $\Delta B_{\Lambda\Lambda}$ would not be satisfied. Hence our event, NAGARA, has been interpreted uniquely as the sequential weak decay of ${}^{6}_{\Lambda\Lambda}He$. Moreover, in the production and decay of ${}^{6}_{\Lambda\Lambda}He$, no particle-stable excited states are known or expected for any of the reaction products. Therefore, there are no ambiguities arising from excited states.

The value of $\Delta B_{\Lambda\Lambda}$ is obtained as $0.62^{+}_{-}0.61$ MeV from the decay vertex B of the double-hypernucleus, while its lower limit is determined as $1.08^{+}_{-}0.22$ MeV, from the production point A. These errors also include the uncertainties in the value of the mass of the Ξ^{-} hyperon (0.13 MeV) and the binding energy of ${}^{5}_{\Lambda}He$ (0.02 MeV).

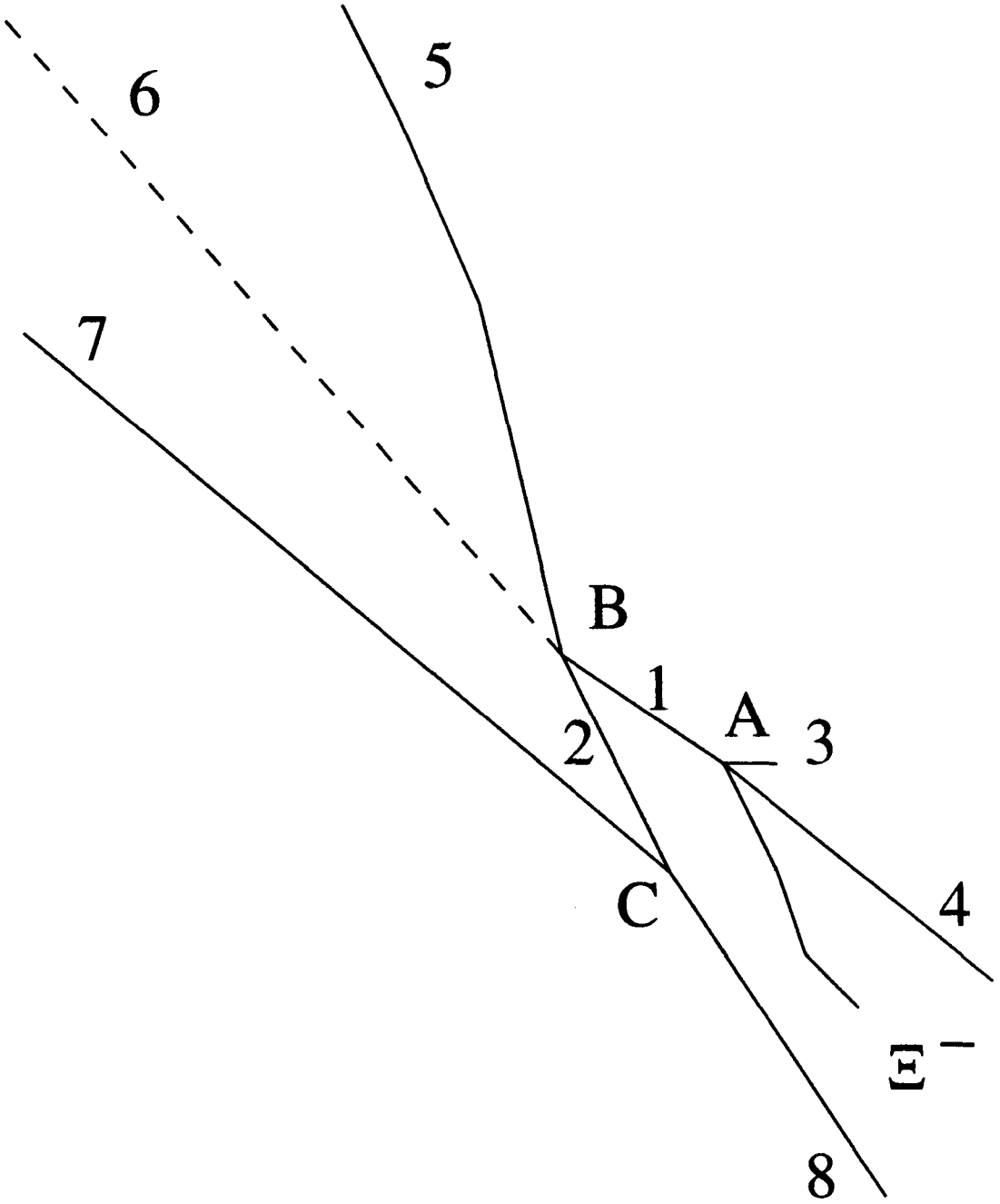

Figure 2.4: Schematic drawing of NAGARA event.

Table 2.1: Lengths and emission angles of the tracks. Angles are expressed by a zenith angle(Θ) with respect to the direction perpendicular to the plate and an azimuthal angle (ϕ). The indicated errors are the measurement errors only.

point	track	length(μm)	θ(degree)	ϕ(degree)	
A	1	8.1$\pm$0.3	44.9$\pm$2.0	337.5$\pm$1.8	double-hypernucleus
	3	3.2$\pm$0.4	57.7$\pm$5.2	174.9$\pm$2.9	
	4	88.3$\pm$0.5	156.2$\pm$0.5	143.0$\pm$1.0	
B	2	9.1$\pm$0.3	77.7$\pm$1.6	115.9$\pm$0.8	single-hyprnucleus
	5	82.1$\pm$0.6	122.8$\pm$1.0	284.2$\pm$0.7	
	6	13697	81.1$\pm$0.8	305.5$\pm$0.1	
C	7	742.6$\pm$0.6	138.5$\pm$0.2	322.1$\pm$0.3	
	8	5868$\pm$20	52.2$\pm$1.2	123.7$\pm$0.7	

Table 2.2: Possible production modes of the double-Λ hypernucleus. The errors on the mass of Ξ^- hyperon and the binding energies of single-hypernuclei are not included in the errors on $B_{\Lambda\Lambda}$ and $\Delta B_{\Lambda\Lambda}$. Only the cases of $\Delta B_{\Lambda\Lambda} < -20$ MeV are listed.

Target	1	3	4	no. of neutrons	$B_{\Lambda\Lambda}$(MeV)	$\Delta B_{\Lambda\Lambda}$(MeV)
^{12}C	${}^{6}_{\Lambda\Lambda}He$	${}^{4}_{\Lambda}He$	p	2n	$>$ 16.9	$>$ 10.6
^{12}C	${}^{6}_{\Lambda\Lambda}He$	${}^{4}_{\Lambda}He$	d	1n	14.5$\pm$0.7	8.2$\pm$0.7
^{12}C	${}^{6}_{\Lambda\Lambda}He$	${}^{4}_{\Lambda}He$	t		7.3$\pm$0.2	1.1$\pm$0.2
^{12}C	${}^{7}_{\Lambda\Lambda}He$	${}^{4}_{\Lambda}He$	p	1n	21.6$\pm$1.3	13.3$\pm$1.3
^{12}N	${}^{6}_{\Lambda\Lambda}He$	${}^{7}_{\Lambda}Li$	p	1n	24.4$\pm$2.1	18.2$\pm$2.1
^{12}N	${}^{6}_{\Lambda\Lambda}He$	${}^{6}_{\Lambda}Li$	d	1n	25.8$\pm$1.3	19.6$\pm$1.3
^{12}N	${}^{6}_{\Lambda\Lambda}He$	${}^{4}_{\Lambda}He$	${}^{4}_{\Lambda}He$	1n	17.9$\pm$1.5	11.7$\pm$1.5
^{12}N	${}^{7}_{\Lambda\Lambda}He$	${}^{4}_{\Lambda}He$	t	1n	26.2$\pm$0.9	17.2$\pm$0.8
^{12}N	${}^{9}_{\Lambda\Lambda}He$	p	${}^{4}_{\Lambda}He$	1n	31.5$\pm$1.8	17.9$\pm$1.8
^{12}O	${}^{8}_{\Lambda\Lambda}He$	${}^{4}_{\Lambda}He$	${}^{4}_{\Lambda}He$	1n	31.1$\pm$0.9	19.9$\pm$0.9

Table 2.3: Possible decay modes of the double hyperfragment which include ${}_{\Lambda}He$ as a decay daughter. The errors on $B_{\Lambda\Lambda}$(MeV) and $\Delta B_{\Lambda\Lambda}$(MeV) do not include those of the binding energies of single-hypernuclei. Only the cases of $\Delta B_{\Lambda\Lambda} > -20$ MeV are listed.

double hypernucleus	2	5	6	no. of neutrons	$B_{\Lambda\Lambda}$(MeV)	$\Delta B_{\Lambda\Lambda}$(MeV)
${}^{5}_{\Lambda\Lambda}He$	${}^{4}_{\Lambda}He$	p	π^-		7.1 ± 0.5	2.4 ± 0.5
${}^{6}_{\Lambda\Lambda}He$	${}^{5}_{\Lambda}He$	p	π^-		6.9 ± 0.6	0.6 ± 0.6
${}^{7}_{\Lambda\Lambda}He$	${}^{5}_{\Lambda}He$	p	π^-	1n	< 8.6	< 0.3
${}^{7}_{\Lambda\Lambda}He$	${}^{6}_{\Lambda}He$	p	π^-		6.3 ± 0.7	-2.0 ± 0.7
${}^{8}_{\Lambda\Lambda}He$	${}^{5}_{\Lambda}He$	p	π^-	2n	< 6.8	< -7.2
${}^{8}_{\Lambda\Lambda}He$	${}^{5}_{\Lambda}He$	p	π^-	1n	< 7.4	< -6.6
${}^{8}_{\Lambda\Lambda}He$	${}^{5}_{\Lambda}He$	p	π^-	1n	< 6.6	< -7.4
${}^{8}_{\Lambda\Lambda}He$	${}^{5}_{\Lambda}He$	p	π^-		7.7 ± 0.8	-6.3 ± 0.8
${}^{9}_{\Lambda\Lambda}He$	${}^{5}_{\Lambda}He$	p	π^-	3n	< 7.2	< -7.1
${}^{9}_{\Lambda\Lambda}He$	${}^{5}_{\Lambda}He$	d	π^-	2n	< 8.2	< -6.1
${}^{9}_{\Lambda\Lambda}He$	${}^{5}_{\Lambda}He$	t	π^-	1n	< 11.2	< -3.1
${}^{9}_{\Lambda\Lambda}He$	${}^{6}_{\Lambda}He$	p	π^-	2n	< 7.2	< -7.1
${}^{9}_{\Lambda\Lambda}He$	${}^{6}_{\Lambda}He$	d	π^-	1n	< 8.4	< -5.9
${}^{9}_{\Lambda\Lambda}He$	${}^{7}_{\Lambda}He$	p	π^-	1n	< 11.2	< -3.1
${}^{9}_{\Lambda\Lambda}He$	${}^{7}_{\Lambda}He$	d	π^-	1n	13.4 ± 0.5	-0.9 ± 0.5
${}^{9}_{\Lambda\Lambda}He$	${}^{8}_{\Lambda}He$	p	π^-	1n	6.4 ± 0.8	-7.9 ± 0.8

Chapter 3

The Hamiltonian

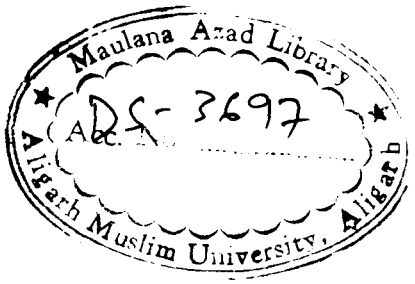

A Hamiltonian H is the observable corresponding to the total energy of the system. A full non-relativistic Hamiltonian (H) of the A-baryon double-Λ hypernucleus is written as

$$H = H_{NC} + H_{\Lambda_1} + H_{\Lambda_2} + v_{\Lambda_1\Lambda_2} \tag{3.1}$$

where, H_{NC} is the non-strange nuclear core Hamiltonian

$$H_{NC} = T_{NC} + \sum_i v_{ij} + \sum_{i<j<k} v_{ijk}, \tag{3.2}$$

H_{Λ_k} is the Hamiltonian arising due to individual Λ

$$H_{\Lambda_k} = T_{\Lambda_k} + \sum_i v_{\Lambda_k} i + \sum_{i<j<k} v_{ijk} \tag{3.3}$$

and $v_{\Lambda_1\Lambda_2}$ is the $\Lambda\Lambda$ potential. Oviously, $H_{NC} + H_{\Lambda_k}$ is Hamiltonian for $A-1$ baryon single-Λ hypernucleus. Now, here we are going to describe different types of baryon-baryon potential which are used in this Hamiltonian. In the study of A baryon single-Λ hypernuclei we use as input ΛN, dispersive ΛNN and NN potentials but in case of A baryon double-Λ hypernuclei instead of these potentials we also include $\Lambda\Lambda$ potentials.

3.1 ΛΛ Potential

3.1.1 Three-Range Gaussian form of ΛΛ Potential

It is considered to be close to realistic potential which fits $^1S_0$ channel phase shift as given by realistic Nijmegen models . It has the form [15, 16] :

$$v_{\Lambda\Lambda}(r) = v_1\ exp\left[-\left(\frac{r}{\beta_1}\right)^2\right] + \gamma\, v_2\ exp\left[-\left(\frac{r}{\beta_2}\right)^2\right] + v_3\ exp\left[-\left(\frac{r}{\beta_3}\right)^2\right] \tag{3.4}$$

The strength v_i (in MeV) and range β_i (in MeV) parameters of the potential simulating $\Lambda\Lambda$ $^1S_0$ Nigmegen interactions are $v_1 = -21.49$, $v_2 = -379$, $v_3 = 9324$ and $\beta_1 = 1.342$, $\beta_2 = 0.777$, $\beta_3 = 0.350$ respectively, with $\gamma = 0.5463$ (NSC97e), $\gamma = 1$(ND), $\gamma = 0.4672$ (NSC00) of Nijmegen models. The dimensionless quantity γ distinguishes amongst various Nigmegen potential models.

3.1.2 Urbana-type ΛΛ Potential

The phenomenological central spin-independent Urbana-type potential has the form

$$v_{\Lambda\Lambda}(r) = v_c(r) - v_0^{\Lambda\Lambda} T_\pi^2(r) \tag{3.5}$$

where, $v_c(r)$ is a Woods-Saxon repulsive core

$$v_c(r) = W_c\left[1 + exp\left(\frac{r-R}{a}\right)\right]^{-1}, \tag{3.6}$$

with $W_c = 2137$ MeV, $R = 0.5$ fm, $a = 0.2$ fm. $T_\pi^2(r)$ is the one-pion exchange tensor potential shape modified with a cut-off:

$$T_\pi(r) = \left(1 + \frac{3}{x} + \frac{3}{x^2}\right)\frac{e^{-x}}{x}\left(1 - e^{-cx^2}\right)^2, \tag{3.7}$$

with x=0.75, $c = 2$ fm^{-2} and $v_0^{\Lambda\Lambda} = -6.1$ MeV is the singlet strength parameter to be obtained from a fit to $B_{\Lambda\Lambda}$ of ${}^{6}_{\Lambda\Lambda}He$. This form of potential was used by Bodmer and Usmani [29], Shoeb et al. [30] in the study of Λ- and ΛΛ-hypernuclei.

3.2 ΛN Potential

The ΛN forces are generated by the exchange (emission or absorption) of mesons, a process to great extent akin to NN forces with the Λ particle having isospin $T_\Lambda = 0$; a single pion cannot be exchanged between Λ particle and a nucleon N, hence one-pion exchange (OPE)

$$\Lambda \rightarrow \Lambda + \pi$$

contribution does not arise for the ΛN interaction because strangeness is also a good quantum number for strong interaction. However, the two-pions exchange (TPE)

$$\Lambda \rightarrow \Sigma + \pi \rightarrow \Lambda + \pi + \pi,$$

or more pion exchange generate the long-range two-body ΛN force. The exchange of K meson, produced in the Yukawa interaction

$$\Lambda \rightarrow N + K^-,$$

give rise to additional short-range forces. In additional to the pion- and K-mesons there are other more massive mesons e.g. the η (548 MeV)- , ω (782 MeV)-mesons etc. which contribute to the short-range ΛN force.

Two-pion exchange (TPE) is a dominant part of the ΛN potential that in turn is mainly determined by the strong tensor one-pion exchange (OPE) component acting twice. Moreover, there is K-exchange interaction that primarily contributes to the ΛN-exchange potential. The tensor part of the ΛN interaction is very weak because the shorter range $\bar{K}$- and K^*-exchange that are responsible for this are of positive sign and nearly cancel each other. (In the case of the NN interaction the π-exchange and ρ-exchange tensor components do not cancel so completely, because their masses are quite different).

We use an Urbana-type [31] potential with spin- and space-exchange components and a TPE tail which is consistent with Λp scattering below the Σ threshold

$$v_{\Lambda N}(r) = v_0(r)(1 - \varepsilon + \varepsilon p_x) + (\frac{V_\sigma}{4})T_\pi^2(r)\sigma_\Lambda \cdot \sigma_N, \tag{3.8}$$

where,

$$v_0(r) = v_c(r) - \bar{v}T_\pi^2(r) \tag{3.9}$$

where, $v_c(r)$ is Woods-Saxon repulsive potential given by Eq. (3.6), $T_\pi(r)$ is the OPE tensor potential given by Eq. (3.7), $x = \mu r$, $\mu = 0.7$ fm^{-1} is the pion mass, and the cut-off parameter $c = 2.0$ fm^{-2} respectively. P_x is the space-exchange operator and ϵ is the corresponding exchange parameter. The $v = (v_s + 3v_t)/4$ and $v_\sigma = v_s - v_t$ are, respectively, the spin-average and spin-dependent strengths, with $v_{s(t)}$ the singlet (triplet) state depths. The various parameters are

$v_s = 6.33$ MeV, $v_t = 6.1$ MeV, $\epsilon = 0.3$,

$W_c = 2137$ MeV, $R = 0.5$ MeV, $a = 0.2$ fm.

These parameters are consistent with the low energy Λp scattering data that essentially determine the spin-average potential $\bar{v}$. The parameter ϵ for the space-exchange strength is fairly well determined from the Λ single-particle scattering data [32].

3.3 ΛNN Potential

The ΛN force as obtained by fitting the Λp scattering does not provide a good account of the experimental binding energies for hypernuclei $A \geq 5$ that are almost a factor of 2 too large.

To resolve overbinding problem, we use a three-body ΛNN interaction. We consider two types of Wigner type ΛNN potentials that arises from projecting out Σ, Δ, etc., degrees of freedom from a coupled channel formalism. These are the dispersive and the TPE ΛNN potentials designated as $V_{\Lambda NN}^D$ and $V_{\Lambda NN}^{2\pi}$, respectively Fig. 3.1. In Urbana model, the three-body ΛNN potential can be written as

$$V_{\Lambda NN} = V_{\Lambda NN}^D + V_{\Lambda NN}^{2\pi} \tag{3.10}$$

$V_{\Lambda NN}^D$ is expected to be repulsive, and phenomenological form of these two are given by

$$V_{\Lambda NN}^D = W_0 T_\pi^2(r_{i\Lambda}) T_\pi^2(r_{j\Lambda})[1 + \frac{1}{6}\sigma_\Lambda \cdot (\sigma_i + \sigma_j)] \tag{3.11}$$

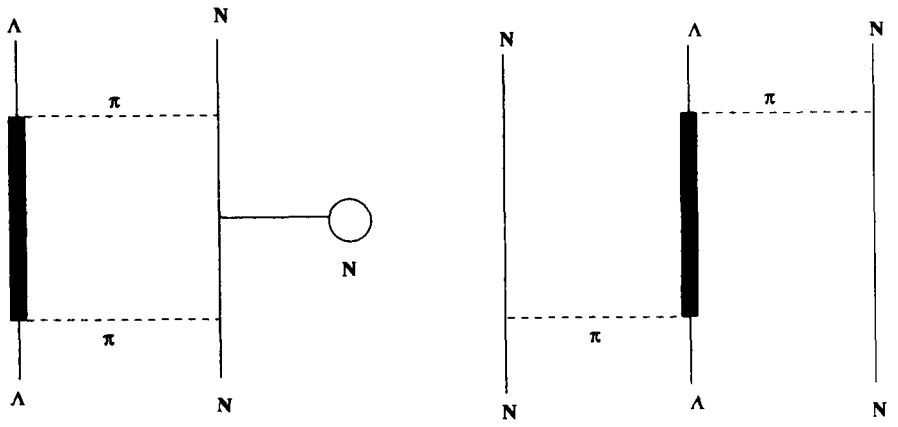

Figure 3.1: Terms contributing to $V^{D}_{\Lambda NN}$ and $V^{2\pi}_{\Lambda NN}$.

where, W_0 is the strength of the potential and $T^2_\pi(r_{i\Lambda})$ is given by Eq.(3.9). $V^{2\pi}_{\Lambda NN}$ consists of two parts corresponding to p- and s-wave $\pi\Lambda$ interactions [33]

$$V^{2\pi}_{\Lambda NN} = W_p + W_s \tag{3.12}$$

where,

$$W_p = -\left(\frac{C_p}{6}\right)(\tau_i \cdot \tau_j)\{X_{i\Lambda}, X_{j\Lambda}\}, \tag{3.13}$$

$$W_s = C_s Z(\mu r_{i\Lambda}) Z(\mu r_{j\Lambda}) \sigma_i \cdot r_{i\Lambda} \sigma_j \cdot r_{j\Lambda} \tau_i \cdot \tau_j, \tag{3.14}$$

$$Y_\pi = \frac{e^{-\mu_\pi r}}{\mu_\pi r}\left(1 - e^{-cr^2}\right), \tag{3.15}$$

$$\{A, B\} = AB + BA, \tag{3.16}$$

$$X_{i\Lambda} = (\sigma_i \cdot \sigma_\Lambda) Y_\pi(r_{i\Lambda}) + S_{i\Lambda} T_\pi(r_{i\Lambda}), \tag{3.17}$$

and

$$Z(x) = \frac{x}{3}[Y_\pi(x) - T_\pi(x)]. \tag{3.18}$$

Here $X_{i\Lambda}$ is the one-pion exchange operator, and $S_{i\Lambda}$ is the tensor operator. The component W_s is quite weak and as in previous studies, we neglect it here.

There are theoretical as well as phenomenological estimates for C_p; but for W_0 the estimates are purely phenomenological. For example, for $W_0 \approx 0.02$, the reduction in the Λ binding to nuclear matter (using central correlations) is approximately in accord

with the suppression obtained in coupled channel ($\Lambda N \rightarrow \Sigma N$) reaction matrix calculation. For C_p theoretical estimates give 1-2 MeV; however, the phenomenological values may not lie in this region as the results depend sensitively on the cut-off parameter c that appear in Eq.(3.9).

3.4 NN Potential

Over the past few decades much information about nucleon-nucleon (NN) interaction has been obtained. It is generally believed that the long range part of NN interaction is due to one-pion exchange since the pion is lightest of all the mesons that couple to the nucleons, its small mass is related to the chiral symmetry of the QCD Lagrangian. At intermediate distances the exchange of multiple pions, with the possible excitation of nucleon resonances like the $\Delta(1232)$, becomes important. At short range, the exchange of heavier mesons and quark-quark interaction may start to dominate. We are still far from a quantitative understanding of NN interaction from the fundamental theory of QCD, however several realistic potential models have been developed in the past decades, based on experimental data and theoretical guidance. Among these models are Reid [34], Paris [35], Urbana [31], and new Argonne V_{18} [36]. The two-body interaction described by these models have common features such as short-range repultion, intermediate-range attraction and long-range one-pion exchange potential (OPEP). Since the one-pion exchange potential (OPEP) is fairly well understood, the two-body potential can be conveniently written as

$$V_{ij} = V_{ij}^{\pi} + V_{ij}^{R} \tag{3.19}$$

where, V_{ij}^{R} denotes the rest of the potential besides the OPEP V_{ij}^{π}. In the nonrelativistic limit, i.e., for slow nucleons,

$$V_{ij}^{\pi}(r) = \frac{f_{\pi NN}^2}{4\pi}\frac{\mu_{\pi}}{3} X_{ij}(\tau_i \cdot \tau_j), \tag{3.20}$$

$$X_{ij}^{\pi} = Y_{\pi}(r_{ij})\sigma_i \cdot \sigma_j + T_{\pi}(r_{ij})S_{ij}, \tag{3.21}$$

where, μ_π is the pion mass, $f_{\pi NN}$ is the pion coupling constant, σ_i, τ_i are the pion and isospin of nucleon i, and S_{ij} is the tensor operator:

$$S_{ij} = 3\sigma_i \cdot \hat{r_{ij}}\sigma_j \cdot \hat{r_{ij}} - \sigma_i \cdot \sigma_j, \tag{3.22}$$

$Y_\pi(r)$ and $T_\pi(r)$ are the Yukawa and tensor functions. In the Urbana-Argonne models they are cut-off at small r with Gaussian cut-off $c = 2.1$ fm^{-2} to take into account the finite size of pions and nucleons:

$$Y_\pi = \frac{e^{\mu_\pi r}}{\mu_\pi r}\left(1 - e^{-cr^2}\right),$$

$$T_\pi(r) = \left(1 + \frac{3}{\mu_\pi r} + \frac{3}{\mu_\pi r^2}\right) Y_\pi(r)\left(1 - e^{-cr^2}\right). \tag{3.23}$$

In addition to the long-range part given by equation (3.20), pion exchange interaction has a short-range part which becomes a δ- function in r_{ij} in the limit of point particles. The δ- function is probably spread out by the finite size of the nucleons, and we include it in V_{ij}^R. The V_{ij}^R may contain heavier meson exchange, multi-pion exchange and quark exchange interaction, and is primarily determined by fitting the NN scattering data.

It is necessary to include at least 14 isoscalar terms in the V^R to fit the data accurately:

$$V_{ij}^R = \sum_{p=1,14} v_p(r_{ij}) O_{ij}^P. \tag{3.24}$$

In the Urbaba-Argonne models the 14 operators are chosen as:

$O_{ij}^{P=1,14} = 1, \tau_i \cdot \tau_j, \sigma_i \cdot \sigma_j, (\sigma_i \cdot \sigma_j)(\tau_i \cdot \tau_j), S_{ij}, S_{ij}(\tau_i \cdot \tau_j), L \cdot S, L \cdot S(\tau_i \cdot \tau_j),$

$L^2, L^2(\tau_i \cdot \tau_j), L^2(\sigma_i \cdot \sigma_j), L^2(\sigma_i \cdot \sigma_j)(\tau_i \cdot \tau_j), L \cdot S^2, L \cdot S^2(\tau_i \cdot \tau_j).$

The static part of V_{ij} containing the first six terms of equation (3.24) dominates, however, the non static part is not negligible and gives rise to spin-orbit splitting in nuclei.

3.5 NNN Potential

The exact calculations of nuclear ground state have shown that two-body potential alone are insufficient to obtain observed binding energies of light nuclei. The inclusion

of three-body potential is of particular importance in the study of nuclear ground states since there is large cancellation between kinetic energy and the two-body potential energy. In the Urbana IX model, the three-body potential can be written as:

$$V_{ijk} = V_{ijk}^{2\pi} + V_{ijk}^{D} \tag{3.25}$$

where, long-range part $V_{ijk}^{2\pi}$ is the attractive two-pion exchange three-nucleon interaction first studied by Fujita-Miyazawa:

$$V_{ijk}^{2\pi} = \sum_{cyc} A_{2\pi} \left(\{X_{ij}, X_{jk}\}, \{\tau_i \cdot \tau_j, \tau_j \cdot \tau_k\} + \frac{1}{4}[X_{ij}, X_{jk}], [\tau_i \cdot \tau_j, \tau_j \cdot \tau_k] \right) \tag{3.26}$$

where,

$$X_{ij} = (\sigma_i \cdot \sigma_j) Y_\pi(r_{ij}) + S_{ij} T_\pi(r_{ij}) \tag{3.27}$$

and square brackets represent the commutator

$$[A, B] = AB - BA.$$

The Fujita-Miyazawa term assesses contribution from diagram such as Fig. 3.2 where, two-pion excite and deexcite a delta resonance. The second term, V_{ijk}^{D} is purely phenomenological. It is assumed to be spin independent and of intermediate range:

$$V_{ijk}^{D} = \sum_{cyc} U_0 T_\pi^2(r_{ij}) T_\pi^2(r_{jk}). \tag{3.28}$$

The parameter $A_{2\pi}$ and U_0 are adjusted to produce the binding energy of light nuclei and equilibrium density of nuclear matter. The resulting value of $A_{2\pi}$ is very close to the Fujita-Miyazawa value.

The three-nucleon interaction is much weaker than the two-nucleon interaction, however, it enhances the tensor correlations slightly and therefore cannot be treated as a first-order perturbation in accurate calculations. Hamiltonian containing two- and three-nucleon interactions accurately reproduce the binding energy of ^4He, thus it seems that four-nucleon interactions are not very important in the nuclear Hamiltonian.

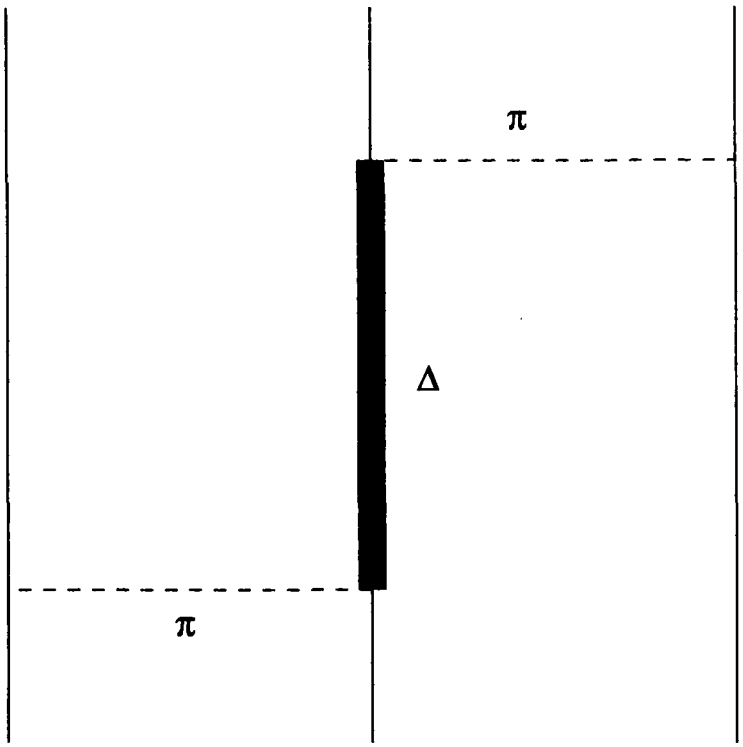

Figure 3.2: Diagram illustrating two-pion exchanged three-body (NNN) interaction.

Chapter 4

Variational Wave Function

Any two-body function can be represented as a correlation operator acting on an uncorrelated state. We can generalize this idea to multiparticle wave function by writing our wave function as a product of correlation operators acting on an uncorrelated state Φ

$$\Psi_\nu = (S\Pi_{i<j}F_{ij})\Phi \tag{4.1}$$

where, F_{ij} is two-body correlation operator, which induces correlations according to the operators in our interaction, Φ is an antisymmetric Staler determinant of single particle state and $S\Pi$ indicates a symmetryzed product over pairs. In general, the F_{ij}'s must be symmetric to maintain the antisymmetric behaviour of the over all wave function Ψ_ν. When $A \leq 4$, Φ is just the spatially independent Staler determinant of the spin- and isospin-state. For example, Φ for ^4He is given by

$$\begin{vmatrix} n\uparrow & n\downarrow & p\uparrow & p\downarrow \\ n\uparrow & n\downarrow & p\uparrow & p\downarrow \\ n\uparrow & n\downarrow & p\uparrow & p\downarrow \\ n\uparrow & n\downarrow & p\uparrow & p\downarrow \end{vmatrix}. \tag{4.2}$$

For $A \geq 5$, spatial dependence must be included in the correlated state Φ in order to obtain a fully antisymmetric wave function. Φ is chosen to be independent of the

center of mass so that Ψ_ν has no center of mass motion.

Variational Wave Function for A-Baryon Hypernucleus:

We are considering A-baryon hypernucleus containing l number of Λ baryons, and $A-l$ number of nucleons[17]. For ΛN space-exchange correlation functions $f_s^l(r)$ and $f_t^l(r)$, one solves the following Schrödinger equation

$$[-\frac{\hbar^2}{2\mu}\nabla^2 + \tilde{v}_{s(t)}^l(r) + \theta_{\Lambda N}(r) + \frac{\hbar^2 l(l+1)}{2\mu r^2}]f_{s(t)}^l(r) = o, \tag{4.3}$$

with the help of quenched ΛN potentials in singlet and triplet states:

$$\tilde{v}_s^l(r) = [v_c(r) - \alpha_{2\pi}\bar{v}T_\pi^2(r)](1 - \varepsilon + \varepsilon p_x^l) + (3/4)\alpha_\sigma v_\sigma T_\pi^2(r), \tag{4.4}$$

$$\tilde{v}_t^l(r) = [v_c(r) - \alpha_{2\pi}\bar{v}T_\pi^2(r)](1 - \varepsilon + \varepsilon p_x^l) - (1/4)\alpha_\sigma v_\sigma T_\pi^2(r), \tag{4.5}$$

where,

$$\begin{aligned}\theta_{\Lambda N} &= \frac{\hbar^2}{2\mu_{\Lambda N}}\left(\kappa_{\Lambda N}^2 - \frac{2\kappa_{\Lambda N}(\nu_{\Lambda N}-1)}{r} + \frac{\nu_{\Lambda N}(\nu_{\Lambda N}-1)}{r^2}\right) \\ &\times \left(1 - exp(-\frac{r^2}{c_{\Lambda N}^2})\right) + \frac{\gamma_{\Lambda N}}{1 + exp(\frac{r-R_{\Lambda N}}{a_{\Lambda N}})}\end{aligned} \tag{4.6}$$

where, $p_x^l \equiv p_x$ is a Majorana space-exchange operator whose value is 1(-1) for $l = 0(1)$ and ε is the corresponding space-exchange strength. The $\alpha_{2\pi}$ and α_σ are quenching parameters of the two-pion and spin-exchange parts of the potential. The $\bar{v} = (v_s + 3v_t)/4$ and $v_\sigma = v_s - v_t$ are, respectively the spin-average and spin-dependent strengths, with $v_{s(t)}$ the singlet (triplet) state depths. $T_\pi(r)$ is the one-pion exchange (OPE) tensor potential and $\theta_{\Lambda N}(r)$ is an auxiliary potential that ensures the asymptotic behaviour of long-range correlation function $f_{s(t)}^l \sim r^{-\nu}e^{-\kappa r}$ [37, 38]. μ is the reduced mass of Λ and N.

Using the above radial solutions f_s^l and f_s^l, we obtain l dependent spin-averaged correlation function

$$f_{\Lambda N}^l(r) = \frac{f_s^l(r) + 3f_s^l(r)}{4}. \tag{4.7}$$

The $f_{\Lambda N}^c(r) = f_{\Lambda N}^0(r)$ is the ΛN central repulsive correlation function with no SEC. In the presence of SEC,

$$u_{\Lambda N}^x(r) = \frac{f_{\Lambda N}^0(r) - f_{\Lambda N}^l(r)}{2}, \tag{4.8}$$

correlation function $f^c_{\Lambda N}(r)$ is modified as

$$f^c_{\Lambda N}(r) = \frac{[f^0_{\Lambda N}(r) + f^l_{\Lambda N}(r)]}{2} = f^0_{\Lambda N}(r) - u^x_{\Lambda N}(r). \tag{4.9}$$

The weak spin-spin correlation function is written as

$$u^x_{\Lambda N}(r) = \frac{[f^0_s(r) - f^0_t(r)]}{4}.$$

The variational wave function written with SEC for A-baryon s-shell hypernucleus with l number of Λ baryons, and $A-l$ number of nucleons:

$$\begin{aligned} |\Psi> \;=\; & \left[1 + U^3 + \sum_{i<j}^{A-l} U^{LS}_{ij}\right]\left[\prod_{j=1}^{A-l}(1 + u^\sigma_{\Lambda j})\right]\left[S\prod_{i<j}^{A-l}(1+U_{ij})\right]\Psi_J \\ & + \frac{1}{\Lambda_p}\sum_{\lambda=1}^{l}\sum_{n=1}^{A-l}\left[1+U^3\right]\left[S\prod_{j=1}^{A-l}(1+U_{ij})\right]\Psi_J u^x_{\Lambda n} P_x. \end{aligned} \tag{4.10}$$

Here,

$$U^3 = 1 + \sum_{\lambda=1}^{l}\sum_{j<k}^{A-l} U_{\lambda jk} + \sum_{i<j<k}^{A-l}(U_{ijk} + U^{TNI}_{ijk}) \tag{4.11}$$

and

$$\begin{aligned} \Psi_J \;=\; & \left[\prod_{\lambda=1}^{l}\prod_{j<k}^{A-l} f^c_{\lambda jk}\right]\left[\prod_{\lambda=1}^{l}\prod_{j=1}^{A-l} f^c_{\lambda j}\right]\left[\prod_{\lambda=1}^{l-1} f^c_{\Lambda\lambda}\right] \\ & \left[\prod_{i<j<k}^{A-l} f^c_{ijk}\right]\left[\prod_{i<j}^{A-l} f^c_{ij}\right]\chi^\sigma_\Lambda \Psi_{JT} \end{aligned} \tag{4.12}$$

Where, U_{ij}, U^{LS}_{ij}, U_{ijk}, U^{TNI}_{ijk} are the non commuting two- and three-baryon correlation operators (Subscripts i, j, k and n stand for nucleons and λ for Λ baryons.). Functions $u^x_{\Lambda i}P_x$ and $u^\sigma_{\Lambda i}\sigma_\Lambda.\sigma_N$ [39] are SEC and spin-spin ΛN correlations. S is the symmetrization (antisymmetrization) operator and Λ_p is the number of ΛN pairs. $\chi^\sigma_\Lambda = A|\downarrow\Lambda\uparrow\Lambda>$ is appropriate antisymmetrized spin wave function for l number of Λ baryons coupled to total angular momentum zero. The $f^c_{\lambda jk}$ is a three-body ΛNN correlation [37]. The $\Lambda\Lambda$ correlation function ($f^c_{\Lambda\Lambda}$) is obtained by solving the Schrödinger equation with phase equivalent Nigmegen potential $v_{\Lambda\Lambda}$ along with an auxiliary potential involving many asymptotic parameters originally defined in Ref. [38].

Removing correlations due to Λ in the above equations, we get s-shell nucleus WF [40, 41]. The second term in Eq. (4.10) is purely due to SEC where, p_x operation (exchange of space position between Λ and N) is made over ΛN pairs: $\sum_{\lambda=1}^{l} \sum_{n=1}^{A-l}$. In order to make the WF translationally invariant, all the positions of baryons are measured from the c.m. of the system as

$$R_{c.m.} = \frac{[m_N \sum_{i=1}^{A-l}(r_i) + m_\Lambda \sum_{\lambda=1}^{l}(r_\lambda)]}{[(A-l)m_N + lm_\Lambda]}, \tag{4.13}$$

$$\tilde{r} = r - R_{c.m.}. \tag{4.14}$$

A p_x operation leads the system to new baryon configuration (r_x) and shifts the c.m. to a new position ($R'_{c.m.}$) by $\Delta R_{c.m.} = R'_{c.m.} - R_{c.m.}$. In order to keep the c.m. unaltered after such an operation, we make a translational shift in all the positions of exchanged configurations

$$\tilde{r}' = r_x - R'_{c.m.} = \tilde{r}_x - R_{c.m.} + \Delta R_{c.m.} \tag{4.15}$$

Chapter 5

Variational Monte Carlo Method

Variational Monte Carlo makes use of a variational wave function and Monte Carlo technique to perform the multidimensional integrals required to evaluate expectation value of ground state of few-body (A=3, 4, 5) nuclear systems. The problem to be solved is the many-body nonrelativistic Schrödinger's equation

$$H\Psi_0 = \left(\sum_i \frac{P_i^2}{2m_i} + \sum_{i<j} V_{ij} + \sum_{i<j<k} V_{ijk}\right)\Psi_0 = E_0\Psi_0, \tag{5.1}$$

where, Ψ_0 is our many-body ground state wave function. Solving this equation for Ψ_0 quickly becomes daunting task as we move from two to three or four nucleons. We can introduce a variational wave function, Ψ_ν and evaluate expectation value in configuration space of the following form

$$\langle\hat{O}\rangle = \frac{\int dR\Psi_\nu^\dagger(R)\hat{O}\Psi_\nu(R)}{\int dR\Psi_\nu^\dagger(R)\Psi_\nu(R)}, \tag{5.2}$$

where, $R = (r_1, r_2....)$ is the multidimensional position vector for all of the particles in nucleus. Such integrals have $3A$-dimensions, equation (5.2) have $3A$-dimensional integral is computationally impossible. In particular, we evaluate the expectation value of the Hamiltonian to determine the variational energy. The parameters of variational wave function are varied to minimize the energy expectation value. This process encompasses the technique of Variational Monte Carlo (VMC).

5.1 Variational Monte Carlo Technique

We use variational method for the approximate determination of the lowest or ground state energy of a system

$$E_0 \leq \frac{\int \Psi^\dagger H \Psi d\tau}{\int |\Psi|^2 d\tau}, \tag{5.3}$$

or expectation value of any operator of the form

$$\langle \hat{O} \rangle = \frac{\int dR \Psi_\nu^\dagger \hat{O} \Psi_\nu}{\int dR \Psi_\nu^\dagger \Psi_\nu} \tag{5.4}$$

contains the multidimensional integral on the right side. Since direct integration is computationally prohibitive, therefore, Monte Carlo method is used to evaluate the expectation values as follows.

The trial wave function or the variational wave function as given by equation (4.1) contains the symmetrized product of two-body correlations. Each order operators in $S\Pi_{i<j}(1 + U_{ij})$ are denoted by p or q. Thus Ψ_q is that component of Ψ in which the operators act in the order p. Expectation values are given by

$$\langle \hat{O} \rangle = \frac{\sum_{p,q} \int dR \Psi_p^\dagger(R) \hat{O} \Psi_q(R)}{\sum_{p,q} \int dR \Psi_p^\dagger(R) \Psi_q(R)}. \tag{5.5}$$

The Monte Carlo integration of equation (5.5) is facillitated i.e. can be made easier by introducing a probability distribution $W_{p,q}(R)$, which approximates the distribution presented by the wave funtion

$$\langle \hat{O} \rangle = \frac{\sum_{p,q} \int dR \frac{\Psi_p^\dagger(R) \hat{O} \Psi_q(R)}{W_{pq}} W_{pq}}{\sum_{p,q} \int dR \frac{\Psi_p^\dagger(R) \Psi_q(R)}{W_{pq}} W_{pq}}. \tag{5.6}$$

The probability function is usually taken to be,

$$W_{p,q}(R) = \Psi_p^\dagger(R) \Psi_q(R), \tag{5.7}$$

however, simple Ψ might be used in $W_{p,q}(R)$ to reduce the computational effort. The crux of the Monte Carlo integration (5.5) is to stochastically sample the probability distribution $W_{p,q}(R)$ and obtain the collection of N uncorrelated or independent configuration, R_i using mean value theorem. The central idea of Monte Carlo evaluation

of integral is that the integral may be estimated by a sum

$$\langle g(x)\rangle = \int_{-\infty}^{\infty} g(x)f(x)dx = E\left(1/N\sum_{i=1}^{N} g(x)\right). \tag{5.8}$$

The method of using the relation given is as follows, draw a series of random variable, x_n from $f(x)$; evaluate $g(x)$ for each x_n. The arithmetic mean of all the values of g is an estimate of the integral, and the variance of this estimate decreases as the number of terms increases. As $N \to \infty$, central limit theorem of probability shows that there is a specific limit distribution for the observed values of g namely, the normal distribution. Using mean value theorem, as $N \to \infty$ equation (5.5) can be reduced to sum over independent configuration as follows:

$$\langle \hat{O} \rangle = \frac{\frac{1}{N}\frac{\sum_i^N \Psi_p^\dagger(R_i)\hat{O}\Psi_q(R_i)}{W_{pq}(R_i)}}{\frac{1}{N}\frac{\sum_i^N \Psi_p^\dagger(R_i)\Psi_q(R_i)}{W_{pq}(R_i)}} \tag{5.9}$$

Since we can not evaluate an infinite number of samples, our expectation value, $\langle \hat{O} \rangle$ has a sampling error which we approximate as the standard deviation σ. We have a relation

$$\sigma^2 = Var\,(\hat{O}) \tag{5.10}$$

i.e.

$$\sigma = \left[\frac{\langle \hat{O}^2 \rangle - \langle \hat{O} \rangle^2}{N-1}\right]. \tag{5.11}$$

Various techniques for sampling probability distribution (i.e., composition of random variable, rejection technique, multivariate distribution and M(RT)^2 algorithm) can be found in Kalos and Whitelock [42]. The technique of great utility in sampling complicated distributions such as in our work is the M(RT)^2 algorithm i.e. Metropolish technique developed by Metropolish, Rosenbluth, Teller and Teller [43]. The steps in the Metropolish algorithm are outlined below:

1. We begin with a set of particle positions R, operater orders p and q; and the corresponding weight $W_{p,q}(R)$.

2. A new point R' is generated from R by randomly moving each particle within a step size l.

$$x_i' = x_i + (\xi_1 - 1/2)l,$$
$$y_i' = y_i + (\xi_2 - 1/2)l,$$
$$z_i' = z_i + (\xi_3 - 1/2)l,$$

where each ξ_i is a random number between 0 and 1. New operator orders, p' and q' are randomly generated and the weight $W_{p'q'}(R')$ of new configuration is constructed.

3. The ratio of the new weight to the old weight is compared to a random number between 0 and 1. If the ratio is greater than the random number, the new configuration is accepted otherwise, the old is regarded as the new configuration.

4. This process (step 2-3) is repeated several times untill an independent configuration is generated. In other words, auto correlation is minimized up to satisfaction. The step size is l, is adjusted such that 50% of the configurations are accepted. If the step size is too small, most of the step will be accepted, but the full configuration space will not be adequately sampled. If the step size is too big, most of the step will be outside the nucleus and thus will be rejected; and once again the distribution will be inadequately sampled.

Chapter 6

Results and Discussion

6.1 Variational Energies

The important energies which we wish to calculate are defined as follows: (i) the separation energy of two Λ hyperons from the core nucleus of ${}^{6}_{\Lambda\Lambda}He$,

$$B_{\Lambda\Lambda} = \frac{\langle \Psi_{A-2}|H_{NC}|\Psi_{A-2}\rangle}{\langle \Psi_{A-2}|\Psi_{A-2}\rangle} - \frac{\langle \Psi_{A}|H|\Psi_{A}\rangle}{\langle \Psi_{A}|\Psi_{A}\rangle}, \tag{6.1}$$

(ii) the separation of a single Λ from the same core nucleus of ${}^{5}_{\Lambda}He$,

$$B_{\Lambda} = \frac{\langle \Psi_{A-2}|H_{NC}|\Psi_{A-2}\rangle}{\langle \Psi_{A-2}|\Psi_{A-2}\rangle} - \frac{\langle \Psi_{A-1}|H_{NC}+H_{\Lambda_1}|\Psi_{A-1}\rangle}{\langle \Psi_{A-1}|\Psi_{A-1}\rangle}, \tag{6.2}$$

(iii) the incremental energy

$$\Delta B_{\Lambda\Lambda} = B_{\Lambda\Lambda} - 2B_{\Lambda}, \tag{6.3}$$

(iv) and the rearrangement energy (E_R) also known as nuclear core polarization (NCP) which is the difference of the internal energy of $(A-l)$ subsystem and the energy of an identical isolated bound nucleus

$$NCP = E_R = E^{int}_{NC} - E_{{}^{4}He} \tag{6.4}$$

where,

$$E^{int}_{NC} = T^{int}_{NC} + V_{NC} \tag{6.5}$$

with

$$T_{NC}^{int} = \sum_{i=1}^{A-l} \frac{p_i^2}{2m_N} - \frac{\left(\sum_{i=1}^{A-l} p_i\right)^2}{2(A-l)m_N} \equiv T_{NC} - T_{NC}^{c.m.}. \tag{6.6}$$

Here, $T_{NC}^{c.m.}$ is the kinetic energy due to c.m. motion of the subsystem around the c.m. of the hypernucleus. The variational energy of the ${}^{5}_{\Lambda}He$ hypenucleus, $E_{{}^{5}_{\Lambda}He} = \frac{\langle\Psi_{A-1}|H_{NC}+H_{\Lambda_1}|\Psi_{A-1}\rangle}{\langle\Psi_{A-1}|\Psi_{A-1}\rangle}$, is taken from Ref. [17], which is obtained using the Hamiltonian, $H_{NC} + H_{\Lambda_1}$, and the Wave function (WF) given by Eq. 4.10 with $l = 1$ and without correlations that arise due to the presence of second Λ hyperon. The basic ingredients used are the two- and three-baryon potential strengths. These, we take the same as in Ref. [17]. For ε=0.1, the ΛN potential strengths: $\bar{v}$=6.15 MeV and v_σ=0.24 MeV together with the ΛNN potential strengths: W^S=0.15 MeV, W^P=0.75 MeV and W^D=0.0193 MeV are found to reproduce the experimental Λ-separation energy (B_Λ^{exp}=3.12(2) MeV). As reported in Ref. [17], we use the result: $\partial W^D/\partial\varepsilon \approx$-0.017 MeV, in order to obtain B_Λ^{exp} for any value of ε. Thus, for ε=0.1, 0.2 and 0.3 respectively, the values of W^D that reproduce B_Λ^{exp} turn out to be 0.0193 MeV, 0.0176 MeV and 0.0158 MeV. Using these potential strengths for $S = -1$ sector along with the Nijmegen (ND) model $\Lambda\Lambda$ potential, we perform calculations for ${}^{6}_{\Lambda\Lambda}He$ in order to obtain variational energy $E_{{}^{6}_{\Lambda\Lambda}He} = \frac{\langle\Psi_A|H\Psi_A\rangle}{\langle\Psi_A|\Psi_A\rangle}$. We use full WF including SEC. We observe that the WF needs to be retuned afresh with any change in the potential strengths. The optimal correlation functions so obtained are plotted in Fig. 6.1, where $f^c_{\Lambda N}(r)$, $u^x_{\Lambda N}(r)$ and $f^c_{\Lambda\Lambda}(r)$ with SEC are represented by solid, dashed and long dashed lines, respectively. Curves with chain and dotted lines represent $f^c_{\Lambda N}(r)$ and $f^c_{\Lambda\Lambda}(r)$ with no SEC. We then switch off SEC in the WF, which is equivalent of ignoring second term in the WF and retuning its variational parameters for an independent energy calculation. In this case, we note a linear dependence: $\partial v_{\Lambda_i}/\partial\varepsilon = \partial E_\Lambda/\partial\varepsilon = \partial E/\partial\varepsilon = -\partial B_\Lambda/\partial\varepsilon \approx$5.0 MeV as in case of ${}^{5}_{\Lambda}He$, where this slope is about 2.3 MeV. This is half of the present value. This may be attributed to the number of ΛN pairs which is twice in case of ${}^{6}_{\Lambda\Lambda}He$ compared to ${}^{5}_{\Lambda}He$. We note that WF remains constant with the variation of ε. All the results of the energy calculation both with and with no SEC are reported in Table 1. One may easily extract SEC effects to every individual piece of energy

Table 1: Energy breakdown for ${}^{6}_{\Lambda\Lambda}$He. Except for ϵ all quantities are in units of MeV. Subsripts i, j and k refer to nucleons and λ refer to Λ hyperons.

		$\epsilon = 0.1$			$\epsilon = 0.2$			$\epsilon = 0.3$	
	(*SEC*)	(No *SEC*)		(*SEC*)	(No *SEC*)		(*SEC*)	(No *SEC*)	
	A	B	A-B	C	D	C-D	E	F	E-F
$T_\lambda = T_{\Lambda_1} + T_{\Lambda_2}$	22.51(6)	21.08(3)	1.43(4)	21.73(6)	21.08(6)	0.65(4)	21.62(6)	21.08(6)	0.54(4)
$v_0(r)(1-\epsilon)$	-33.67(8)	-32.65(5)	-1.02(7)	-29.31(7)	-29.02(7)	-0.29(7)	-25.38(6)	-25.39(6)	0.01(6)
$v_0(r)\epsilon P_x$	-3.24(1)	-3.14(1)	-0.10(1)	-6.37(2)	-6.27(2)	-0.10(1)	-9.48(3)	-9.41(3)	-0.07(4)
$(\frac{1}{4})v_\sigma T^2_\pi(r)\sigma_\lambda \cdot \sigma_i$	0.06(0)	0.046(0)	0.014(0)	0.06(0)	0.046(0)	0.014(0)	0.05(0)	0.046(0)	0.004(0)
$v_{\lambda i}$	-36.84(9)	-35.74(6)	-1.10(7)	-35.62(9)	-35.25(8)	-0.37(7)	-34.83(9)	-34.75(8)	-0.08(7)
$v_{\Lambda\Lambda} = v_{\Lambda_1\Lambda_2}$	-5.99(5)	-4.65(5)	-1.34(7)	-5.51(5)	-4.65(5)	-0.86(7)	-5.49(5)	-4.65(5)	-0.84(7)
$V^D_{\lambda ij}$	6.08(2)	5.65(1)	0.43(1)	5.61(2)	5.15(2)	0.46(1)	4.99(2)	4.65(2)	0.34(2)
$V^P_{\lambda ij}$	-4.81(2)	-5.71(2)	0.90(3)	-4.97(2)	-5.71(2)	0.74(3)	-4.75(2)	-5.71(2)	0.96(3)
$V^S_{\lambda ij}$	-0.05(0)	-0.049(1)	-0.001(1)	-0.01(0)	-0.049(0)	0.039(2)	-0.05(0)	-0.049(0)	-0.001(2)
$V^{2\pi}_{\lambda ij} = V^P_{\lambda ij} + V^S_{\lambda ij}$	-4.86(2)	-5.75(2)	0.89(3)	-4.97(2)	-5.75(2)	0.78(3)	-4.80(2)	-5.75(2)	0.95(3)
$V_{\lambda ij} = V^D_{\lambda ij} + V^{2\pi}_{\lambda ij}$	1.22(2)	-0.11(1)	1.33(2)	0.64(2)	-0.60(2)	1.24(2)	0.19(2)	-1.10(2)	1.29(3)
$V_\lambda = v_{\lambda i} + v_{\lambda\lambda} + V_{\lambda ij}$	-41.52(9)	-40.50(8)	-1.02(8)	-40.50(9)	-40.50(8)	0.00(8)	-40.13(9)	-40.50(8)	0.37(8)
$E_\Lambda = T_\lambda + V_\lambda$	-19.01(5)	-19.42(4)	0.41(6)	-18.77(5)	-19.42(5)	0.65(6)	-18.51(5)	-19.42(5)	1.01(6)
T_{NC}	121.05(16)	119.32(15)	1.73(21)	119.94(15)	119.32(15)	0.62(21)	119.91(15)	119.32(15)	0.59(21)
v_{NN}	-131.75(14)	-129.43(14)	-2.32(21)	-130.95(14)	-129.43(14)	-1.52(21)	-131.04(14)	-129.43(14)	-1.61(21)
V_{NNN}	-5.58(2)	-5.18(2)	-0.40(3)	-5.52(2)	-5.18(2)	-0.34(3)	-5.63(2)	-5.18(2)	-0.45(3)
$V_{NC} = v_{ij} + V_{ijk}$	-137.33(15)	-134.61(15)	-2.72(21)	-136.47(15)	-134.61(14)	-1.86(21)	-136.67(15)	-134.61(14)	-2.06(21)
$E_{NC} = T_{NC} + V_{NC}$	-16.29(6)	-15.29(4)	-1.00(6)	-16.53(4)	-15.29(4)	-1.24(6)	-16.76(4)	-15.29(4)	-1.47(6)
$E_{{}^{6}_{\Lambda\Lambda}\mathrm{He}} = E_\lambda + E_{NC}$	-35.30(5)	-34.72(2)	-0.58(3)	-35.30(5)	-34.72(4)	-0.58(3)	-35.27(5)	-34.72(4)	-0.56(3)
$B_{\Lambda\Lambda}$	7.57(5)	6.99(4)	0.58(3)	7.57(5)	6.99(4)	0.58(3)	7.57(5)	6.99(4)	0.58(3)

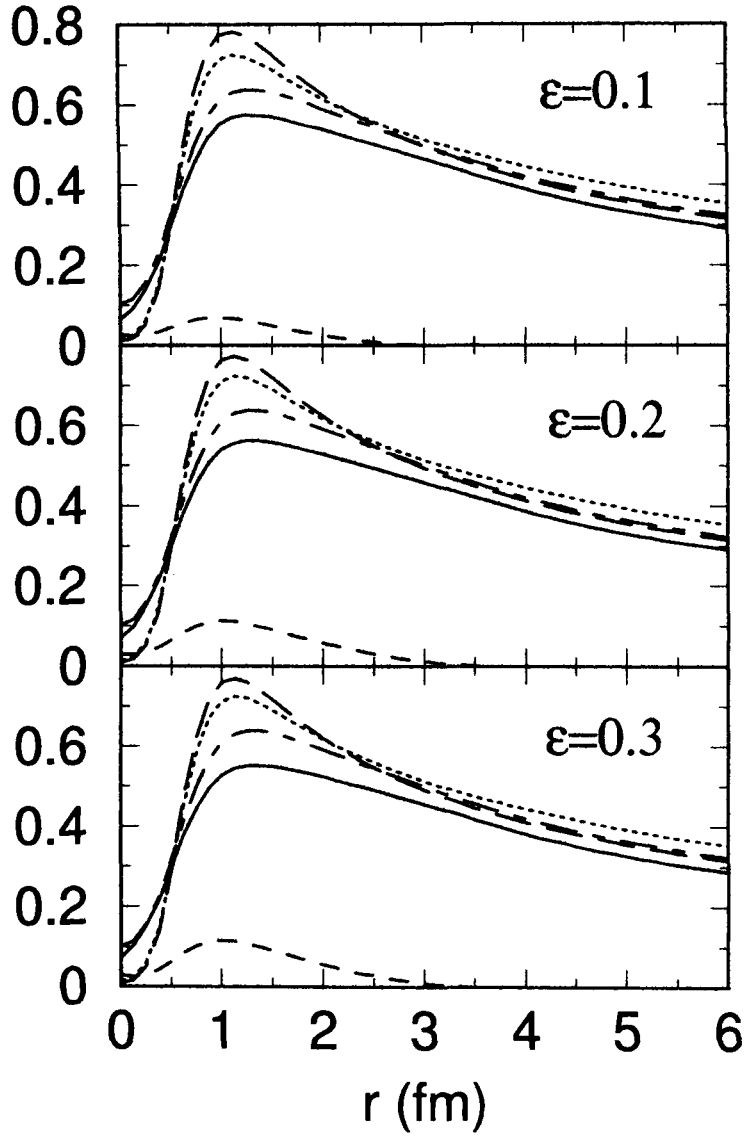

Figure 6.1: The solid, dashed and long dashed lines represent $f^c_{\Lambda N}(r)$, $u^x_{\Lambda N}(r)$ and $f^c_{\Lambda\Lambda}(r)$ with *SEC*. The chain and dotted lines represent $f^c_{\Lambda N}(r)$ and $f^c_{\Lambda\Lambda}(r)$ with no *SEC*

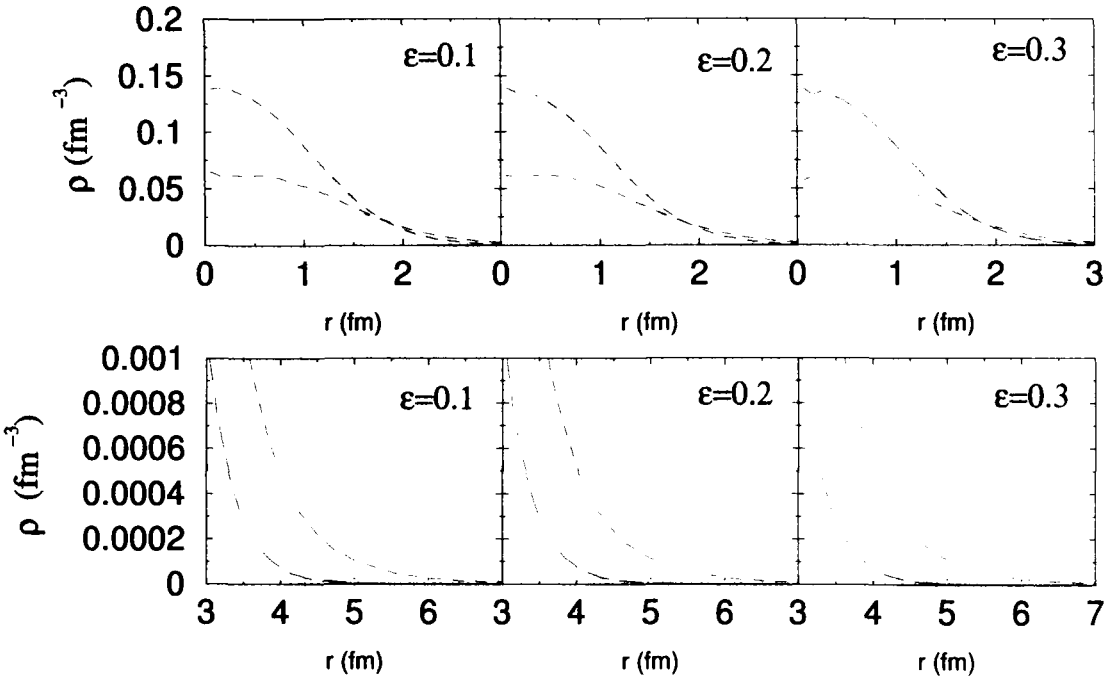

Figure 6.2: The dashed and long dashed lines represent Λ and p densities in ${}^{6}_{\Lambda\Lambda}He$ with blue and green colors for SEC and no SEC. Yellow filled circles show p in ${}^{4}He$.

breakdown from this Table. Although each and every piece of energy breakdown is significantly affected with the variation of ε with the SEC in the WF, the energies calculated using Nijmegen equivalent ND model of $\Lambda\Lambda$ potential along with other three sets of strengths for ε =0.1, 0.2 and 0.3 used in the $S = -1$ sector that reproduce B_Λ^{exp} of ${}^{5}_{\Lambda}He$ converge to the same value $B_{\Lambda\Lambda}$ ≈7.57(5) MeV of ${}^{6}_{\Lambda\Lambda}He$ within the small statistical uncertainties. This value of $B_{\Lambda\Lambda}$ is close to the experimental value $B_{\Lambda\Lambda}^{exp}$ =7.25(19) MeV, which may well be reproduced through a little variation in γ used in $v_{\Lambda\Lambda}$. Thus, we note an important result that the set of two- and three-body potential strengths that reproduces experimental B_Λ^{exp} of ${}^{5}_{\Lambda}He$ also reproduces experimental $B_{\Lambda\Lambda}^{exp}$ of ${}^{6}_{\Lambda\Lambda}He$. This gives confidence in the fully correlated WF [17] and hope for the resolution of $A = 5$ anomaly [44, 45, 46]. This is because of the linear behaviours, $\partial B_{\Lambda\Lambda}/\partial\varepsilon = c_1$ and $\partial V^D_{\Lambda ij}/\partial W^D = \partial E_{{}^{6}_{\Lambda\Lambda}He}/\partial W^D = -\partial B_{\Lambda\Lambda}/\partial W^D = c_2$, (Here, c_1 and c_2 are positive constants.), which lead to the same linear dependence between ε and W^D: $\partial W^D/\partial\varepsilon \approx$-0.017 MeV as in the case for ${}^{5}_{\Lambda}He$. Like ${}^{5}_{\Lambda}He$, the total energy obeys a linear behaviour with ε. Hence, $\partial E_{{}^{6}_{\Lambda\Lambda}He}/\partial\varepsilon = -\partial B_{\Lambda\Lambda}/\partial\varepsilon \approx$constant. The $E_\Lambda = T_\lambda + v_{\lambda i} + v_{\lambda\lambda} + V_{\lambda ij}$ is found decreasing with increasing ε. However, unlike ${}^{5}_{\Lambda}$He it does not obey a linear dependence with ε. Also, the repulsion due to $V^D_{\lambda ij}$ is found decreasing significantly with increasing ε. This is because change in density profiles lead to the change in $T_\pi(r)$. But the attraction offered by $V^P_{\lambda ij}$ exhibits only a little variance, although functions $Y(r)$ and $Z(r)$ too experience a change due to change in density profiles. But they appear with operators which too play a role as $V_{\Lambda ij}$ is sensitive to its own correlation. It is also important to note that the s-wave $V^S_{\Lambda ij}$ is not a negligible quantity. The average $\langle P_x\rangle = \langle v_0(r)\varepsilon P_x\rangle/\langle\varepsilon v_0(r)\rangle$ as extracted from Table 6.1 in case of no SEC is 0.88(1). But with SEC, WF involves another P_x operator.

6.2 Nuclear Core Polarization and Density Profiles

We note a large polarization of nuclear core for both the choices of the WF (i) with (ii) and with no SEC (Table 6.1). The value of NCP with no SEC is found to be 8.86(4) MeV for all the three values of ε as WF remains invariant with the variation

Table 6.1: Nuclear core polarization (NCP).

	${}^{6}_{\Lambda\Lambda}He$		${}^{5}_{\Lambda}He$	
	(SEC)	(No SEC)	(SEC)	(No SEC)
	(MeV)	(MeV)	(MeV)	(MeV)
ε=0.1	8.39(5)	8.86(4)	3.59(4)	4.31(4)
ε=0.2	7.83(5)	8.86(4)	3.16(4)	4.31(4)
ε=0.3	7.57(5)	8.86(4)	2.70(4)	4.31(4)

of ε. However with SEC, it is found to be 8.39(5) MeV, 7.83(5) MeV and 7.57(5) MeV for ε=0.1, ε =0.2 and ε =0.3, respectively. These values are more than twice of the corresponding values of ${}^{5}_{\Lambda}He$. With SEC, NCP decreases with increasing ε, but slightly. Also, in case of ${}^{5}_{\Lambda}He$, we note that more compact is the nuclear core less is the polarization [17]. This slow variation of NCP is perhaps because of the fact that point proton radius of NC does not change to any significant value with the variation of ε. The point proton radius of NC with and with no SEC is found about 1.67(1) fm and 1.71(1) fm, respectively. Its value in case of isolated ${}^{4}He$ is 1.46(1) fm whereas 'experimental' value is 1.47 fm. The significant reduction in point proton radius of NC with SEC leads to reduction in the quadrupole moment (Table 6.2) Hence NC is less deformed with SEC which may be attributed to the pressure. The quadrupole moment of NC is found sensitive to the repulsive ΛNN correlation. Also for ${}^{5}_{\Lambda}He$ and with no SEC, repulsive correlation $f^{c}_{\Lambda N}$ pushes both the nucleons and the Λ towards the periphery and at the centre [37, 39]. But SEC significantly reduces the repulsive correlation in the interior region in the range $r \approx 0.5 - 2.0$ fm. Therfore, both nucleons and Λ recieve an inward pull leading to reduction in peripheral density profiles and enhancement in the interior density profiles Fig. 6.2. As a result, both NC and the hypernucleus are found more compact with SEC which offers a pressure. Similar is the result for ${}^{5}_{\Lambda}He$ where a direct correlation between density profiles and repulsive correlation $f^{c}_{\Lambda N}$ was noticed. However, features are more prominent in case of ${}^{6}_{\Lambda\Lambda}He$

Table 6.2: Point proton radius and quadrupole moment of nuclear core (NC)

	point proton radius		Quadrupole moment	
	(SEC)	(No SEC)	(SEC)	(No SEC)
	(fm)	(fm)	(fm^2)	(fm^2)
ε=0.1	1.666(1)	1.710(1)	0.006(1)	0.020(1)
ε=0.2	1.678(1)	1.710(1)	0.015(1)	0.020(1)
ε=0.3	1.667(1)	1.710(1)	0.005(1)	0.020(1)

obviously because of the presence of two Λ hyperons.

This study confirms the conclusions drawn in case of ${}^{5}_{\Lambda}He$ that SEC significantly affects every physical observable. These effects manifest more with increasing quantum of strangeness. Hence, inclusion of SEC for any realistic calculation is inevitable. We also note that $B_{\Lambda\Lambda}$ obtained with Nijmegen ND model potential is quite close to the experimental value. The s-wave ΛNN potential though small is not a negligible quantity. We note a large polarization of NC, which is found deformed with the presence of two Λ hyperons. However, deformation reduces due to SEC. Point proton radius and NCP also get reduced due to SEC.

Bibliography

[1] M. Danysz and J. Pniewski, Phil. Mag. **44** , 348 (1953)

[2] A.Gal, Adv. Nucl. Sci. **8**, 1, (1977).

[3] M. Danysz et al. Nucl. Phys. **49** , 121 (1963).

[4] D. J. Prowse, Phys. Rev. Lett. **17** , 782 (1966).

[5] S. Aoki et al., Prog. Theor. Phys. **85**, 1287 (1990).

[6] S. B. Carr, I. R. Afnan and B. F. Gibson, Nucl. Phys. A **625** 143 (1997).

[7] R. L. Jaffe, Phys. Rev. Lett. **38**, 195 (1977)

[8] H. Takahashi et al., Phys. Rev. Lett **87**, 121502 (2001).

[9] J. K. Ahn et al. Phys. Rev. Lett. **87**, 132504 (2001).

[10] I. N. Filikhin and A. Gal, Phys. Rev. C **707** 491 (2002).

[11] I. N. Filikhin and A. Gal, Phys. Rev. C **65** 041001(R) (2002).

[12] I. N. Filikhin and A. Gal, Phys. Rev. Lett. **89** 172502 (2002).

[13] I. N. Filikhin and A. Gal, V. M. Suslov Phys. Rev. C **68** 024002 (2003).

[14] E. Hiyama, M. Kamimura, T. Motoba, T. Yamada and Y. Yamamoto, Phys. Rev. Lett. **89**, 142508 (2002); Phys. Rev. C **66** 024007 (2002).

[15] M. Shoeb, Phys. Rev. C **69**, 054003 (2004).

[16] Q. N. Usmani, A. R. Bodmer, Bhupali Sharma Phys. Rev. C **70**, 061001 (2004).

[17] A. A. Usmani, submitted to Phys. Rev. C.

[18] A. Nogga, H. Kamada, and W. Glockle, Phys. Rev. Lett. **88**, 172501 (2002).

[19] H. Nemura, Y. Akaishi, and Y. Suzuki, Phys. Rev. Lett. **89**, 142504 (2002).

[20] A. R. Bodmer, Q. N. Usmani and J. Carlson, Nucl. Phys. A **422**, 510 (1984).

[21] R. H. Dalitz, D. H. Davis, P. H. Fowler, A. Montwill, J. Pniewski, and J. A.Z akrzewski, Proc. Roy. Soc. Lond. A **426**, 1 (1989)

[22] C. B. Dover et al., Phys. Rev. C **44**, 1905 (1991).

[23] Y. Yamamoto, H. Takaki and Ikeda, Prog. of Theor. Phys.

[24] M. Danysz et al., Phys. Rev. Lett. **11** , 29 (1963).

[25] S. Aoki et al., Phys. Rev. Lett. **65**, 1729 (1990).

[26] R. H. Dalitz et al., Proc. R. Soc. London A**426**, 1 (1963).

[27] D. H. Davis, J. Pniewski, Contemp. Phy. **27**, 91 (1986).

[28] D. Zhu, C. B. Dover, A. Gal and M. May, Phys. Rev. Lett. **67**, 2268 (1986).

[29] A. R. Bodmer, Q. N. Usmani, Nucl. Phys. A **468** 653 (1987).

[30] M. Shoeb et al., Phys. Rev. C **59** 02807 (1999).

[31] I. E. Lagaris and Pandharipande, Nucl. Phys. A **359** 331 (1981).

[32] Q. N. Usmani, M. Sami, and A. R. Bodmer, in Condensed Matter Theories, edited by J. W. Clark, K. A. Schoeb and A. Sadiq (Novas Science Publishers, Commack, N.Y., Vol. **9**. (1994))

[33] R .K. Bhaduri, B. A. Loiseau and Y. Nogami, Ann. Phys. (N.Y.) **44**, 57 (1967).

[34] R. V. Reid, Jr., Ann. Phys. (N.Y.) **50**, 411 (1968).

[35] M. Lacombe et al., Phys. Rev. C **21** 861 (1980).

[36] R. B. Wiringa, V. G. J. Stoks, R. Schiavilla, Phys. Rev. C **51**, 38 (1995).

[37] A. A. Usmani, S. Murtza, Phys. Rev. C **68**, 024001 (2003).

[38] A. R. Bodmer, Q. N. Usmani, Nucl. Phys. A **477** 653 (1988)

[39] A. A. Usmani, S. C. Pieper, Q. N. Usmani, Phys. Rev. C **51**, 2347 (1995).

[40] A. Arriaga, V. R. Pandharipande and R. B. Wiringa, Phys. Rev. C **52**, 2362 (1995).

[41] B. S. Pudliner, V. R. Pandharipande, J. Carlson, S. C. Pieper and R. B. Wiringa, Phys. Rev. C **56**, 1720 (1997); R. B. Wiringa, Phys. Rev. C **43**, 1585 (1991).

[42] M. H. Kalos and P. Whitelock, Monte Carlo Methods vol-**1**, Basic Willey, New York (1986).

[43] N. Metropolis et al., J. Chem. Phys. **21**, 1087, (1953).

[44] A. Gal, Adv. Nucl. Phys. **8**, 1 (1975).

[45] R. H. Dalitz, R. C. Herndon, and Y. C. Tang, Nucl. Phys. B **47**, 109 (1972).

[46] E. V. Hungerford and L. C. Biedenhorn, Phys. Lett. B **142**, 232 (1984).